2016

Synthesis and Characterization of Curcumin Polymer for Application in Radiation Induced Lung Damage

Mark C. Bailey
University of Kentucky, mba243@g.uky.edu
Digital Object Identifier: http://dx.doi.org/10.13023/ETD.2016.293

STUDENT AGREEMENT:

I represent that my thesis or dissertation and abstract are my original work. Proper attribution has been given to all outside sources. I understand that I am solely responsible for obtaining any needed copyright permissions. I have obtained needed written permission statement(s) from the owner(s) of each third-party copyrighted matter to be included in my work, allowing electronic distribution (if such use is not permitted by the fair use doctrine) which will be submitted to UKnowledge as Additional File.

I hereby grant to The University of Kentucky and its agents the irrevocable, non-exclusive, and royalty-free license to archive and make accessible my work in whole or in part in all forms of media, now or hereafter known. I agree that the document mentioned above may be made available immediately for worldwide access unless an embargo applies.

I retain all other ownership rights to the copyright of my work. I also retain the right to use in future works (such as articles or books) all or part of my work. I understand that I am free to register the copyright to my work.

REVIEW, APPROVAL AND ACCEPTANCE

The document mentioned above has been reviewed and accepted by the student's advisor, on behalf of the advisory committee, and by the Director of Graduate Studies (DGS), on behalf of the program; we verify that this is the final, approved version of the student's thesis including all changes required by the advisory committee. The undersigned agree to abide by the statements above.

Mark C. Bailey, Student

Dr. Thomas Dziubla, Major Professor

Dr. Thomas Dziubla, Director of Graduate Studies

SYNTHESIS AND CHARACTERIZATON OF CURCUMIN POLYMER FOR APPLICATION IN RADIATION INDUCED LUNG DAMAGE

THESIS

A thesis submitted in partial fulfillment of the
requirements for the degree of Master of Science in
Chemical Engineering in the College of Engineering
at the University of Kentucky

By

Mark Cheyne Bailey

Lexington, Kentucky

Director: Dr. Thomas D. Dziubla, Gill Professor, Associate Professor of Chemical Engineering

Lexington, Kentucky

2016

ABSTRACT OF THESIS

SYNTHESIS AND CHARACTERIZATON OF CURCUMIN POLYMER FOR APPLICATION IN RADIATION INDUCED LUNG DAMAGE

Radiotherapy is used as a primary treatment for many cancers, including lung cancer. Although radiotherapy has proven to be an effective cancer treatment, its use is heavily limited due to the peripheral toxicity to healthy tissue. In this work, the antioxidant, curcumin, was tested as a radioprotectant to reduce radiation damage to healthy cells. Curcumin has been limited in use due to its poor bioavailability. In order to avoid problems associated with free curcumin delivery, curcumin poly(beta-amino ester) (CPBAE) was synthesized.

The first study investigated the *in vitro* radioprotection effect of curcumin in HUVEC dosed with gamma radiation. Cells treated with curcumin showed significantly less ROS development compared to both untreated radiated and non-radiated cells. Cells treated with curcumin showed a decrease in viability for both radiated and non-radiated cells. Curcumin pretreatment exhibited no reduction in γ-H2AX foci formation in cells after radiation damage. These results indicate that curcumin does not radioprotect cells in an *in vitro* model.

In a second study, curcumin was polymerized using a Michael addition reaction to create a hydrolytically degradable poly(beta-amino ester). Curcumin multiacrylate and isobutylamine reacted to form curcumin poly(beta-amino ester) (CPBAE). This polymer's chemical structure and properties were characterized and nanoparticles were made from the polymer. Nanoparticles synthesized were able to successfully release curcumin through degradation, but at a low efficiency and extended time scale.

KEYWORDS: Linear Polymer Synthesis, Nanoparticles, Radiation, Antioxidant, Curcumin, Cell Culture

Mark Cheyne Bailey

6/20/16

SYNTHESIS AND CHARACTERIZATON OF CURCUMIN POLYMER FOR APPLICATION IN RADIATION INDUCED LUNG DAMAGE

By
Mark Cheyne Bailey

Dr. Thomas Dziubla,
Director of Thesis

Dr. Thomas Dziubla
Director of Graduate Studies

June 20th, 2016

Table of Contents

List of Tables

List of Figures

Chapter 1: Introduction

Radiation therapy is the targeting and delivery of ionizing radiation at a specific dose to a cancer site. Ionizing radiation is radiation that has enough energy to remove electrons from atoms or molecules causing a change in charge and unpairing electrons. Ionizing radiation comes in many forms including X-rays, gamma rays and high energy ultraviolet rays. All of these sources create free radicals when interfacing with tissue. Most of these free radicals are created from water molecules as they are the greatest constituent of biological material [1]. DNA damage to cancer cells is the primary goal of radiation therapy and it is caused by these free radicals breaking DNA strands. If a cell has sufficient damage done to the DNA, mitotic cell death or apoptosis will occur. Cancer cells are much more sensitive to DNA damage caused by radiation due its destructive effects in dividing cells. Cancer cells divide at a much greater rate than most other healthy cells, making radiation disproportionately more damaging to cancer cells and an effective treatment [2].

Radiation therapy is used to treat many different cancer types including skin cancer, larynx carcinoma, lymphoma, head and neck cancers, prostate cancers, breast cancer, lung cancer and others [3]. Of these, lung cancer is an especially common and aggressive form of cancer, accounting for 13.3% of new cancer cases while also accounting for 26.5% of cancer deaths [4]. Lung cancer is conventionally treated through a combination of chemotherapy and radiotherapy. Treatment could greatly benefit from higher radiation dosing schedules though as higher radiation dose has correlated to higher survival rate in patients with non-small cell lung cancer treated with 3D-CRT radiation [5]. Despite this, radiation dose to the lungs is limited due to radiation induced fibrosis. Higher mean dose of radiation to the lungs increases the volume of fibrosis developed in the lungs and leads to pneumonitis [6]. If this risk of pneumonitis could be

reduced though, higher, more effective radiation doses could be used in treating lung cancer. Considering these factors, protection of healthy endothelial cells during lung cancer treatment was investigated in this work.

This development of pneumonitis first begins will the introduction of excess reactive oxidative species (ROS) created by ionizing radiation. ROS are a natural part of cellular respiration where there is a constant state of developing and scavenging free radicals. Oxidative stress is achieved when the ROS generation exceeds the antioxidant capacity of the system. This results in damage to the cells and elicits other downstream actions, such as inflammation. Inflammation is the body's natural response to harmful stimuli such as pathogens, cellular damage or in this case oxidative stress induced by radiation. Inflammation involves recruitment of leukocytes to the area in the process of wound healing. Acute inflammation recruits leukocytes which work to remove harmful stimuli and progress to restoration of functional tissue [7]. The constant state of oxidative stress created by radiation in endothelial cells is not acute inflammation though, it is characterized as chronic inflammation. Chronic inflammation occurs when the negative stimuli cannot be resolved by the recruited leukocytes. As the initial neutrophils were not able to solve the problem, macrophages are recruited and begin progressive and severe fibrosis to isolate the injury [8]. This severe fibrosis leads to reduced lung capacity, difficulty breathing and in severe cases, mortality for the patient.

When the natural systems at work in the cells are no longer able to handle the oxidative load, supplemental antioxidants are useful to prevent further damage. In order to address this, curcumin was proposed as a radioprotectant of healthy cells during radiation treatment. Curcumin is a natural phenol molecule with anti-oxidant, anti-inflammatory and anti-cancer properties [9]. Curcumin has been shown to be safe in clinical trials, as both free curcumin [10] and in liposomal form [11]. Curcumin has also been shown to interact favorably with NF-KB, a

cellular mechanism which regulates apoptosis in both cancer cells and endothelial cells. Cancer cells are at an elevated expression of NF-KB, curcumin is able to reduce this expression and sensitize them to radiation induced death. In the case of healthy endothelial cells, the downregulation of NF-KB would reduce cell apoptosis and reduce surrounding toxicity.

Curcumin also exhibits limitations as drug including poor aqueous solubility which leads to reduced tissue uptake and bioavailability. This combined with curcumin molecules reducing to metabolites *in vivo* has made it difficult to simply use high dose curcumin as an effective clinical treatment [12]. In theory, low bioavailability can be addressed through developing a nanoparticle delivery system. Poly(beta-amino esters) are a class of polymers that can readily be broken down through hydrolytic degradation. Curcumin PBAE (CPBAE) has been developed and is more stable than free curcumin, being able to achieve a sustained release profile over hours rather than minutes [13, 14]. Linear CPBAE can be formed into a nanoparticle and targeted to the lungs. These particles would ideally be delivered intravenously. Intravenous delivery requires that the nanoparticles are able to circulate in the bloodstream and directly interact with vascular endothelial cells however. Both of these factors are size dependent. Nanoparticles are able to circulate for an extended amount of time in the bloodstream in the 50-500 nm size range [15] and internalize into the endothelium in the 80-500nm size range [16]. Based on these factors and studies of nanoparticle systems in the lungs, an ideal range of size for particles would be 50-400nm [17].

In this work, a model was first developed that induces radiation damage to human umbilical vein endothelial cells *in vitro*. Radiation was shown to increase ROS generation, reduce cell viability and increase γ-H2AX foci formation. Following studies showed curcumin was able to reduce ROS generated from radiation. Curcumin was also shown to further reduce the viability of radiated cells though and had no impact on reducing γ-H2AX foci formation. In a second

study, curcumin was polymerized using a Michael addition reaction to create a linear, hydrolytically degradable poly(beta-amino ester). The linear polymer was successfully formed into nanoparticles. It was found that the polymer released curcumin over a 15 day period.

Chapter 2: Background

2.1 Radiation therapy and mechanism

2.1.1 Ionizing radiation

Ionizing radiation is radiation that has enough energy to remove free electrons from atoms or molecules causing a change in charge and ionizing them. This includes particulate radiation such as α particles, β particles and cosmic rays and photon radiation including X-rays, γ rays and extreme ultra violet radiation [18]. Particulate radiation has the added aspect of kinetic energy that it can directly alter the structure of molecules and proteins while photon ionizing radiation acts solely through removing electrons from molecules.

2.1.2 Ionizing radiation interaction with cells

DNA damage to cancer cells is the primary goal of radiation therapy and it is caused by free radicals breaking DNA strands. Most of these free radicals are created from water molecules as they are the greatest constituent of biological material [1]. When a cell has sufficient damage done to the DNA from free radical damage, mitotic cell death or apoptosis will occur. Cancer cells are much more sensitive to DNA damage caused by radiation due its destructive effects in dividing cells. Cancer cells divide at a much greater rate than most other healthy cells, making radiation disproportionately more damaging to cancer cells and an effective treatment [2].

2.1.3 Ionizing radiation sources

The two types of ionizing radiation conventionally used in radiotherapy are gamma rays and X-rays. Although gamma radiation and x-rays are separately defined on the electromagnetic spectrum, these two types of radiation are conventionally differentiated by how they produced

rather than the characteristics of the emitted radiation. Gamma rays are produced by radioactive decay of materials, where most commonly used materials for medical use are Cobalt-60 and Cesium-137. X-rays on the other hand are produced by electrons being ejected from the shell of an atom. X-rays and gamma rays are both measured for dosing in gray units and intensity of the source is measured in electron volts (eV). A gray unit is defined as one joule of ionizing radiation absorbed in one kilogram of material. The intensity of the source is either proportional to the wavelength on the electromagnetic spectrum if produced as an X-ray or characteristic of the emission of a specific radioactive material [18]. Cobalt-60 has a decay energy of 2.844 MeV while Cesium-137 has a decay energy of 1.176 MeV [19]. As defined by the electromagnetic spectrum, gamma rays occupy shortest wavelength of energy and highest energy at wavelengths less than 10^{-11}m. X-rays occupy the range from 10^{-12}m to 10^{-9}m. There is overlap in this range, and many clinical X-rays use intensities similar to gamma radiation sources [20-23].

2.1.4 Radiation delivery methods

Multiple methods are available for external beam radiation treatment. The first method of delivery developed for treatment was 2D conformal radiation therapy (2D-CRT). 2D-CRT has is directed by a 2D location of the tumor and radiation is delivered from 1 or more points, typically from an X-ray [24]. 2D-CRT delivers the most radiation to surrounding tissue, but is still sees use as palliative treatment for end stage metastatic cancers. 3D conformal radiation therapy (3D-CRT) is more advanced and typically guided by a 3D image of the tumor from a CT scan or MRI. 3D-CRT is the most commonly used form of external beam radiation treatment and is ideal for tumors that are immobile. Stereotactic body radiation therapy (SBRT) is a third method developed for radiation therapy. SBRT is treatment guided and adjusted in real time by a 3D image of the tumor through CT or ultrasound, which allows for high specificity of radiation dose

[25]. SBRT allows for great precision and reduces radiation dose to surrounding tissue due to its high specificity. SBRT has allowed for much more precise treatment of inoperable, moving tumors such as those in the lungs and heart.

2.2 Lung cancer

2.2.1 Lung cancer causes and development

Lung cancer is one of the most understood cancers in terms of epidemiology. It has been linked to carcinogens in smoking as well as exposure to radon gas and pollution [4]. Despite this knowledge, lung cancer continues to be a common and aggressive form of cancer, accounting for 13.3% of new cancer cases while also accounting for 26.5% of cancer deaths [4].

2.2.2 Lung cancer classification

Lung cancer is divided into multiple types and stages. The main two primary types are small-cell lung carcinomas (SCLCs) which make up 10% of diagnoses and non-small cell lung carcinomas (NSCLCs) which encompasses the remaining 90%. SCLC is further divided into small cell carcinoma and combined small cell carcinoma. NSCLC includes squamous cell carcinoma, large cell carcinoma and adenocarcinoma[4]. Stages of lung cancer include formation of cancer (stage I), cancer spreading to lymph nodes (stage II), cancer spreading to lymph nodes in upper bronchus (stage) III and cancer metastasizes outside the lung (stage IV) [26]. 57% of lung cancer is diagnosed once cancer has metastasized, which leads to limited treatment options.

2.2.3 Lung cancer treatment

Lung cancer is difficult to treat with surgery as tumors can not always be removed effectively. This has led to non-invasive treatments of radiation therapy and chemotherapy being the primary treatments for the disease. SCLC is characterized by faster growth and more aggressive progression towards metastasis than NSCLC [27]. Due to having a more aggressive

disease path, SCLC standard treatment involves high dose chemotherapy, high intensity radiation, and multiple cisplatin regiments [28]. NSCLC has a better expected outcome than SCLC and in early stages multiple treatment options are available including thoracoscopic surgery to remove tumors [29].

2.2.4 Radiation induced pneumonitis

Radiation dosing is limited in lung cancer treatment due to increased risk for development of pneumonitis and fibrosis. At higher levels of radiation dose per volume, an increased amount of fibrotic tissue forms in the lungs [30]. This risk of development of fibrosis is measured by mean lung dose and V_{20} [31]. V_{20} is defined as there percentage of volume of the lung receiving 20 Gy of radiation or more. When 2D-CRT and 3D-CRT are employed for treatment, a V_{20} of the patient's lung is kept below 22%, as risk for pneumonitis and fibrosis greatly increases above this threshold [32, 33] Using SBRT, lower fractionalization is used at higher intensities so V_{20} is kept below 7% in clinical treatment to reduce these same risks [34]. The pneumonitis toxicities risk peak at 71 days [33] and it is imperative to reduce these immediate problems, but higher dose radiation is ideal for long term survival for patients with locally advanced NSCLC [5, 35].

2.3 Reactive oxidative species

2.3.1 Reactive oxidative species in cell cycle

Reactive oxidative species (ROS) are naturally occurring elements in cells, produced by mitochondria and other organelles. ROS are radicals that cause DNA damage, protein damage and lipid damage which are naturally produced by cells and scavenged when at equilibrium [35]. Aside from damaging effects at high levels, ROS play an important role in directing cellular differentiation, proliferation, apoptosis and migration [36]. The generation of ROS is a favorable

response to pathogens and other negative stimuli in most cases as it triggers an immune response to resolve the problem.

Oxidative stress occurs when there is an elevated level of free radicals in a system that is not resolved and leads to cellular dysfunction. This can come from sources such as a metabolic disease, neurodegenerative disease or an acute injury such as or radiation damage [37, 38]. Additionally, dysfunctional cells such as cancer cells have been found to be in a constant state of elevated oxidative stress [39].

2.3.2 Antioxidants

Antioxidants are species that are able to scavenge free radicals and reduce the oxidative stress of a system. Antioxidants can either be enzymes or small molecules [40]. They can be produced naturally by the body or derived from alternative sources. Small molecule antioxidants have been of greatest interest as treatments due to their ability to scavenge multiple types of free radicals and simpler delivery.

Antioxidant supplement treatments have been proven effective in multiple studies. The antioxidant H_2 has been shown to effectively reduce radiation induced lung damage [41], Trolox has proven to be an effective antioxidant to suppress nanoparticle induced oxidative stress [42], Quercetin suppresses oxidative stress in multiple models [43, 44], Resveratrol, another potent antioxidant has been applied in many studies [45, 46] and Curcumin has been shown to reduce ROS generation in multiple instances [47-49].

2.4 NF-κB

A major component of curcumin's activity profile is its ability to downregulate NF-kB. [9, 50]. NF-κB is a transcription factor that regulates many cytokines and adhesion molecules [51]. The components of this transcription factor include p50, p52, p65, REL and RELB proteins. These

proteins are phosphorylated in the cytoplasm and migrate to the nucleus where they begin a cascade which results in transcription of DNA, these transcriptions lead to expression of proinflammatory cytokines such as TNF-α and IL-1 [52].

2.5 Inflammation

Inflammation is the body's natural response to pathogen or foreign invasion. Inflammation is characterized by first detection of the foreign invasion through antibody detection, oxidative stress or another cellular indication of pathogen [53].

This is followed by cellular mechanisms such as NF-kB which will express proinflammatory cytokines including IL-1, IL-8 and TNF-α [54]. After expressing these proinflammatory cytokines, endothelial cells will induce expression of cellular adhesion molecules on their surface. Cellular adhesion molecules such as ICAM-1 and VCAM-1 are expressed on the surface of the cell, facilitating the recruitment of leukocytes and macrophages to the site of injury as well as promoting vasodilation [55].

The acute inflammation begins as monocytes and neutrophils are recruited to the site and phagocytose the offending pathogen. If the injury is not able to be resolved, macrophages are recruited to the site. Macrophages act in many roles, including facilitating phagocytosis, increasing local levels of oxidative stress, inducing angiogenesis and producing extracellular matrix [56]. This production of extracellular matrix can be used to encapsulate the foreign body in fibrotic tissue and isolate it from the rest of the body [57]. If the injury is not localized to a discrete object though, widespread fibrosis of the tissue can occur which leads to many chronic inflammatory disease states such as pneumonitis [58].

2.6 Curcumin

2.6.1 Curcumin structure and properties

Curcumin is a natural phenol molecule derived from turmeric known for its anti-oxidant, anti-inflammatory and anti-cancer properties. Curcumin contributes to the orange color of turmeric and has a strong absorption peak at 420 nm. Curcumin is a strong antioxidant [48] and potent anti-inflammatory, downregulating pro-inflammatory cytokines including IL-6, IL-8 and TNFα [59]. Due to these properties, curcumin has been investigated as a chemosensitizer [60, 61], radiosensitizer [62-64] and neuroprotective agent [65, 66]. It has been purported as an anti-cancer drug as well due to anti-angiogenic effects [47], pro-apoptotic effects [67, 68] and anti-proliferative effects [68-70].

High dosing of curcumin is also relatively safe, as no toxicities from an oral dose of curcumin at 12g per day in humans was observed. The limiting factor in maximum oral curcumin dosing was patient compliance [71]. Curcumin has repeatedly exhibited poor bioavailability however, owing to its low absorption in the GI tract, rapid metabolism and rapid elimination [72]. Curcumin has a short half-life *in vivo*, quickly reducing to components [73], 90% of curcumin degrades in 30 minutes at physiological conditions [9].

2.6.2 Curcumin as a radioprotectant

The radio sensitizing effects of curcumin on cancer cells *in vitro* has been observed in multiple studies [62, 74-76]. The radioprotective effect of curcumin is less understood but has been well documented *in vivo* studies. It is thought that the primary mechanism of radiation protection of healthy tissue is reduction of ROS and attenuated inflammatory response. When curcumin was given as oral dose to rats, a reduction of lung fibrosis was observed after full body X-ray radiation of 13.5 Gy [22, 23]. Another study rats which were fed an oral dose of curcumin

had multiple beneficial effects in protecting the ilium mucosa after abdominal gamma radiation of 5 Gy [77]. Rats given oral dose of curcumin showed reduced ROS levels in tissue after 3 Gy full body gamma radiation [78]. Curcumin protected against radiation induced cataracts in rats after 15 Gy full body gamma radiation [79] and administration of liposomal curcumin reduced radiation pneumonitis after 25 Gy X-ray full body radiation [80]. Curcumin has shown to reduce apoptotic cells in rat ovaries after 8.3 Gy of whole body gamma radiation [81]. In human trials where the radiation dose to patients ranged from 42.6–50.4 Gy, oral dose of curcumin has shown to reduce radiation induced dermatitis [82].

2.7 Poly(beta-amino esters)

PBAE are synthesized through an addition reaction between amines and acrylates. This reaction is an energetically favorable process where the acrylate and amine undergo a Michael addition, creating an ester bond between the two molecules. Use of primary amine and diacrylate molecules creates a linear PBAE, while networked polymer is produced from use of multifunctional amine or acrylates in synthesis.

PBAE have been of interest for a variety of applications due to the tune-ability of the polymer class. Hundreds of acrylates and amines can be chosen from to adjust polymer properties such as length, charge, connectivity, degradation properties and toxicity [83, 84]. Linear PBAE have seen significant study in gene delivery due to their cationic properties. The cationic polymer is able to condense anionic DNA into nanoparticles and act as a degradable delivery vehicle[85]. Another area of interest in PBAE is crosslinked gels. These PBAE gels can be tuned to control degradation and have applications as biomaterials [86] and delivery of hydrophobic drugs [87].

In this work curcumin was acrylated to form curcumin multiacrylate. This presents a unique application where the active drug is built into the PBAE delivery vehicle. The active curcumin is preserved until release upon the breaking of the ester bond in the polymer. This PBAE system can then be tuned for degradation properties though selection of primary amines.

Chapter 3: Research Goals

3.1 Introduction

The aim of this thesis was to develop a curcumin nanoparticle system that could be targeted to the lung vasculature through intravenous injection. A radiation injury model was developed and curcumin was tested to determine the amelioration of radiation damage to healthy cells. Curcumin poly(beta-amino ester) was synthesized and characterized in order to understand the chemical makeup and properties. HPLC and GPC was used to determine curcumin content and molecular weight. FTIR was performed to determine molecular components in the polymer. DSC provided insight into the glass transition temperature of the polymer. CPBAE nanoparticles were synthesized and the size stability and degradation properties of these nanoparticles were studied. Oxidative stress plays a critical role in both lung carcinoma and healthy lung cell death. By delivering degradable curcumin nanoparticles to the lungs, oxidative stress in healthy cells may be able to be reduced and toxicity from radiation can be attenuated.

3.2 Objectives and Significance

The overall hypothesis of this work is:

> *Linear curcumin poly(beta-amino ester) polymer can be synthesized and used to form nanoparticles for targeted release of curcumin that scavenge free radicals and influence radiation response of both cancer cells and healthy tissue.*

3.2.1 Specific Aim 1: Develop a radiation damage model and evaluate curcumin's effect on cellular injury

A. Characterize damage to human umbilical vein endothelial cells from gamma radiation developed by a Cs-137 irradiator.

B. Introduce curcumin to radiation damage model and assess change in Calcien AM Orange-Red viability, DCF-DA fluorescence and γ-H2AX foci formation.

3.2.1.1 Hypothesis 1

Using radiation damage model developed, curcumin will reduce oxidative stress in irradiated cells, increasing viability and reducing γ-H2AX foci formation.

3.2.1.2 Significance and Outcome

Experiments outlined and carried out in chapter 4 test this hypothesis. A radiation model protocol was successfully developed that quantified radiation damage to human umbilical vein endothelial cells. Curcumin was shown to reduce the viability of irradiated cells in a dose dependent manner, while trolox at all concentrations tested had no effect of cell viability. Curcumin and trolox were shown to decrease DCF fluorescence after radiation damage indicating reduction in radiation damage. When the cellular response in cells was evaluated in the γ-H2AX foci formation assay, no protection in DNA breaks was found.

3.2.2 Specific Aim 2: Synthesis and characterization of linear CPBAE

A. Synthesize linear CPBAE and characterize using Gel Permeation Chromatography (GPC), High Performance Liquid Chromatography (HPLC), Differential Scanning Calorimetry (DSC) and Fourier Transformed Infrared Spectroscopy (FTIR)
B. Develop CPBAE nanoparticles with size and stability relevant for intravenous drug delivery
C. Characterize degradation of curcumin poly(beta-amino ester) in bulk polymer and in nanoparticles

3.2.2.1 Hypothesis 2

Utilizing a Michael addition reaction between curcumin diacrylate and an amine, curcumin poly(beta-amino ester) can be synthesized into a linear polymer which can degrade and release curcumin to exert therapeutic effect.

3.2.2.2 Significance and Outcome

Experiments outlined and carried out in chapter 5 test this hypothesis. A Michael addition reaction method was used to produce curcumin poly(beta-amino ester). CPBAE composed of CMA and IBA was synthesized and characterized with GPC, HPLC, DSC and FTIR. These tests positively indicated polymerization during the reaction. Nanoparticles were synthesized using the developed CPBAE and were able to be size controlled for the desired application of intravenous delivery. Nanoparticles were found to be stable but degraded very slowly through hydrolysis. Both the CPBAE nanoparticles and bulk CPBAE polymer only released a maximum of 20% of the theoretical yield.

Chapter 4: Curcumin and Effect on Radiation Damage

4.1 Introduction

Radiation oncology has seen significant advances over the past 100 years which have led to better treatment for a variety of cancers including skin cancer, larynx carcinoma, lymphoma, head and neck cancers, prostate cancers, lung cancer and breast cancer [3]. Developments in radiation technology aim to increase the dose of radiation to tumor sites and reduce the amount delivered to surrounding tissue [3]. Recent technologies such as stereotactic body radiation therapy (SBRT) have made radiation dosing even more precise, which has allowed for greater selectivity in treating tumors [88]. Although doses of radiation are now more precise, peripheral toxicities are still the factor that limits the amount of radiation that can be administered [5, 89, 90]. It is still desirable to deliver higher amounts of radiation to better kill tumor cells though [91] and to achieve this end, radioprotectors, molecules that exert a differential protective effect on healthy tissue over cancer cells have been investigated. Amifostine is currently the only radioprotector that has been approved by the FDA for use in this manner [92]. Although Amifostine has seen success in clinical trials [93], there are significant drawbacks including increased nausea, hypotension and limited time of protection for Amifostine after delivery [94, 95].

Curcumin is one molecule that has been of interest for use as a radioprotectant. Curcumin is a natural phenol molecule with anti-oxidant and anti-cancer properties [9]. Curcumin has been shown to be safe in clinical trials, including as free curcumin [10] and delivery in liposomal form [11]. High dosing of curcumin is also relatively safe, as no toxicities from an oral dose of curcumin at 12g per day in humans was observed. Curcumin had a low rate

of uptake in the GI tract and the limiting factor in maximum oral curcumin dosing was patient compliance [71].

Curcumin has been shown to be effective as a radioprotector in multiple studies. When curcumin was given as oral dose to rats, a reduction of lung fibrosis was observed after full body X-ray radiation of 13.5 Gy [22, 23]. Rats which were fed an oral dose of curcumin had multiple beneficial effects in protecting the ilium mucosa after abdominal gamma radiation of 5 Gy [77]. Rats given oral dose of curcumin showed reduced ROS levels in tissue after 3 Gy full body gamma radiation [78]. Curcumin protected against radiation induced cataracts in rats after 15 Gy full body gamma radiation [79] and administration of liposomal curcumin reduced radiation pneumonitis after 25 Gy X-ray full body radiation [80]. Curcumin has shown to reduce apoptotic cells in rat ovaries after 8.3 Gy of whole body gamma radiation [81]. In human trials where the radiation dose to patients ranged from 42.6–50.4 Gy, oral dose of curcumin has shown to reduce radiation induced dermatitis [82].

Curcumin's radioprotective effect is thought to be due to its reduction of oxidative stress and inhibition of transcription of genes related inflammation in healthy cells [96]. Its radiosensitization of cancer cells has been linked to its upregulation of nuclear factor Kappa-Beta (Nf-kB), promoting apoptosis in cancer cells [96]

The radio sensitizing effects of curcumin on cancer cells *in vitro* has been observed in multiple studies [62, 74-76]. The radioprotective effects of curcumin have been demonstrated in both clinical and animal models as described above, but *in vitro* studies have not been as clear cut. Curcumin has not been shown to increases viability of any healthy cell line. In fact, curcumin tends to reduce viability of healthy cells on its own [97]. This indicates that curcumin may not be radioprotecting primarily through antioxidant capacity of curcumin as theory suggests.

4.2 Methods and Materials:

4.2.1 Reagents

All reagents were received and used as delivered. 2', 7'-dichlorodihydrofluorescein diacetate (DCF-DA) was purchased from Invitrogen. Calcien AM red-orange was purchased from life technologies. Single donor HUVECs, EGM-2 culture media and pen-strep was purchased from Lonza. Curcumin was purchased from Chem-Impex International, Inc and trolox was purchased from Sigma Aldrich.

4.2.2 Irradiation Conditions

University of Kentucky radiation facility's Shepherd Model Mark I-30 Cs-137 irradiator was used for dosing cells with radiation. Irradiation was performed at room temperature with rotation to ensure an even dose across well plates. Gamma radiation was delivered at a rate of 4.4 Gy/min to deliver doses ranging from 2-20 Gy.

4.2.3 Cell Culture Preparation Conditions

HUVEC were propagated and cultured at 37°C at 5% CO_2 and 95% Humidity. Lonza EGM-2 culture media with penicillin and streptomycin was changed 24 hours after seeding into a new flask and every 48 hours. HUVEC seeded in well plates had media changed every 48 hours as well unless otherwise specified.

4.2.4 Confluent Cell Viability Model

HUVECs were seeded in a 96 well plate and cultured overnight to confluency. Cells were then irradiated using the Shepherd Model Mark I-30 Cs-137 irradiator and then incubated. A Calcien AM live assay was then performed to assess the viability of the cells at each Time points 0, 1, 2, 3, 5 and 10 days after radiation. Cells were washed twice with warm media followed by the addition of 2µM Calcien AM in Media. The well plate was then incubated for 1 hour. The

wells were then washed twice more in warm media. The fluorescence was read on the Synergy MX plate reader (540 nm excite, 590 nm emission).

4.2.5 Cell Proliferation

HUVECs were seeded in 96 well plates and cultured for 24 hours. The cells were then treated with either free curcumin or free trolox and were incubated for 1 hour. Cells were then irradiated using the Shepherd Model Mark I-30 Cs-137 and cultured for 72 hours. A Calcien AM live assay was then performed to assess the viability of the cells. Cells were washed twice with warm media followed by the addition of 2μM Calcien AM in Media. The well plate was then incubated for 1 hour. The wells were then washed twice more in warm media. The fluorescence was read on a Synergy MX plate reader (540 nm excite, 590 nm emission).

4.2.6 Cell ROS Generation

HUVECs were seeded in 96 well plates at 20,000 cells/cm^2 and cultured for 24 hours. The cells were then treated with 5 μM of DCF-DA and either free curcumin or free trolox. Cells were then incubated for 1 hour. After incubation, the plates were then irradiated using the Shepherd Model Mark I-30 Cs-137 and cultured for 24 hours. Fluorescence reading of the cells was taken at the 24 hour time point after radiation. Plates were read on a Synergy MX plate reader at 485 nm excitation, 530 nm emission.

4.2.7 Cell γ-H2AX foci Formation Assay

HUVEC were seeded in 4 chambered chamber slides at 50,000 cell/cm^2 and incubated for 24 hours. Two chamber slides were then pretreated with 1μg/mL curcumin and incubated for an hour. The other two chamber slides had their media changed. The chamber slides were then incubated for 1 hour. One of the curcumin incubated chamber slide and one with media chamber slide was irradiated at 20 Gy. The chamber slides were then washed in warm PBS once.

A half an hour after radiation, the slides were fixed in 3.7% formaldehyde in PBS for 20 minutes. The chamber slides were then washed twice more in warm PBS. Immunofluorescence staining was then performed and images of cells were taken using fluorescent microscopy.

4.3 Results

4.3.1 Development of Radiation Model

Lung tissue is highly vascularized and endothelial cells are a priority for radiation protection. Endothelial cells are susceptible to oxidative stress and are actively involved in recruiting leukocytes. Due to this, HUVEC were selected as a cellular system to evaluate damage to the healthy endothelium surrounding tumors. No systematic model is present in the literature using these cells to evaluate radiation damage however. The response of these cells to radiation was investigated in order to develop a meaningful assay.

HUVECs were seeded at confluency and treated with 0 Gy, 20 Gy or 40 Gy dose of radiation. Viability of cells was measured over ten days. Viability results were normalized to the percent viability of the 0 Gy control of that day. Only a small difference in viability was seen in irradiated cells at early time points, indicating no acute damage through this Calcien AM viability assay. There was also no observable difference in viability between 20 Gy and 40 Gy irradiated cells as well. Even 5 days after radiation, the radiation groups had 60% of the fluorescence values of non-irradiated cells. This delayed effect on viability was possibly due to cell wash off of irradiated groups and no healthy cells can proliferate to replace them. This data indicates that even at high radiation doses the mechanism of damage to cells is still through reduction of proliferative ability.

In order to observe radiation damage to cells in a proliferative environment, cells were seeded subconfluent at 10,000 cells/cm^2, 20,000 cells/cm^2 and 40,000 cells/cm^2. Cells were then radiated and viability was measured 72 hours later using Calcien AM. No significant difference

between the 20 Gy and 40 Gy irradiated groups was measured, but cells seeded at 10,000 cells/cm^2 had 43% the viability of non-irradiated cells, 20,000 cells/cm^2 had 69% the viability of non-irradiated cells and 40,000 cells/cm^2 had 72% the viability of non-irradiated cells. Although 10,000 cells/cm^2 seeding density showed the greatest difference in viability between irradiated cells and non-irradiated cells, 20,000 cells/cm^2 seeding density was chosen for the radiation model due to highest experimental consistency.

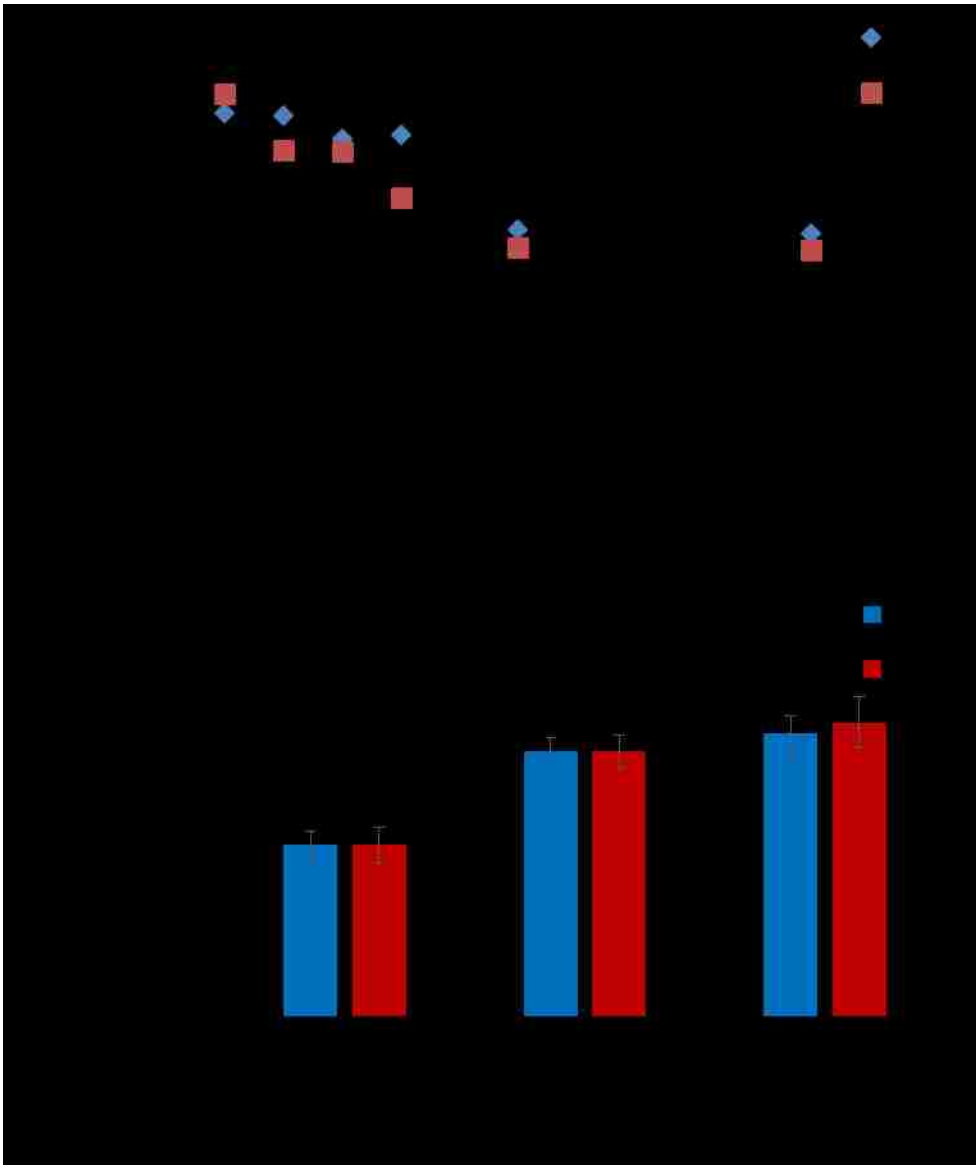

Figure 4-1: HUVEC viability radiation response N=4. Error bars represent standard error. * indicates p-value<0.05 in two-way ANOVA. (A) HUVEC radiation injury model: HUVEC were treated with radiation and normalized to percent of non-irradiated values at each time point (B) HUVEC viability 3 days after radiation as a function of cell seeding density. Control group was considered the group with no radiation for each cell density.

4.3.2 Viability of cells after proliferating

The viability of the proliferating cells were measured to determine the effect antioxidants and radiation had in the model. Antioxidant concentrations ranging from 0-10µg/mL were incubated for 1 hour with cells before radiation. 72 hours after radiation, a

Calcien AM live assay was performed. Cells recieving 20 Gy exhibited 74% viability of non-irradiated cells. Cells treated with trolox had no significant effect on viability as viability remained constant as trolox concentration increased. When cells were pretreated with curcumin, lower viabilities were observed as concentration increased. When cells were treated with both curcumin and radiation the resulting viability was lower than either one individually. This data indicates that curcumin inhibits cell proliferation and it is not a function of its antioxidant capacity as trolox has no effect even at concentrations greatly above 10μg/mL.

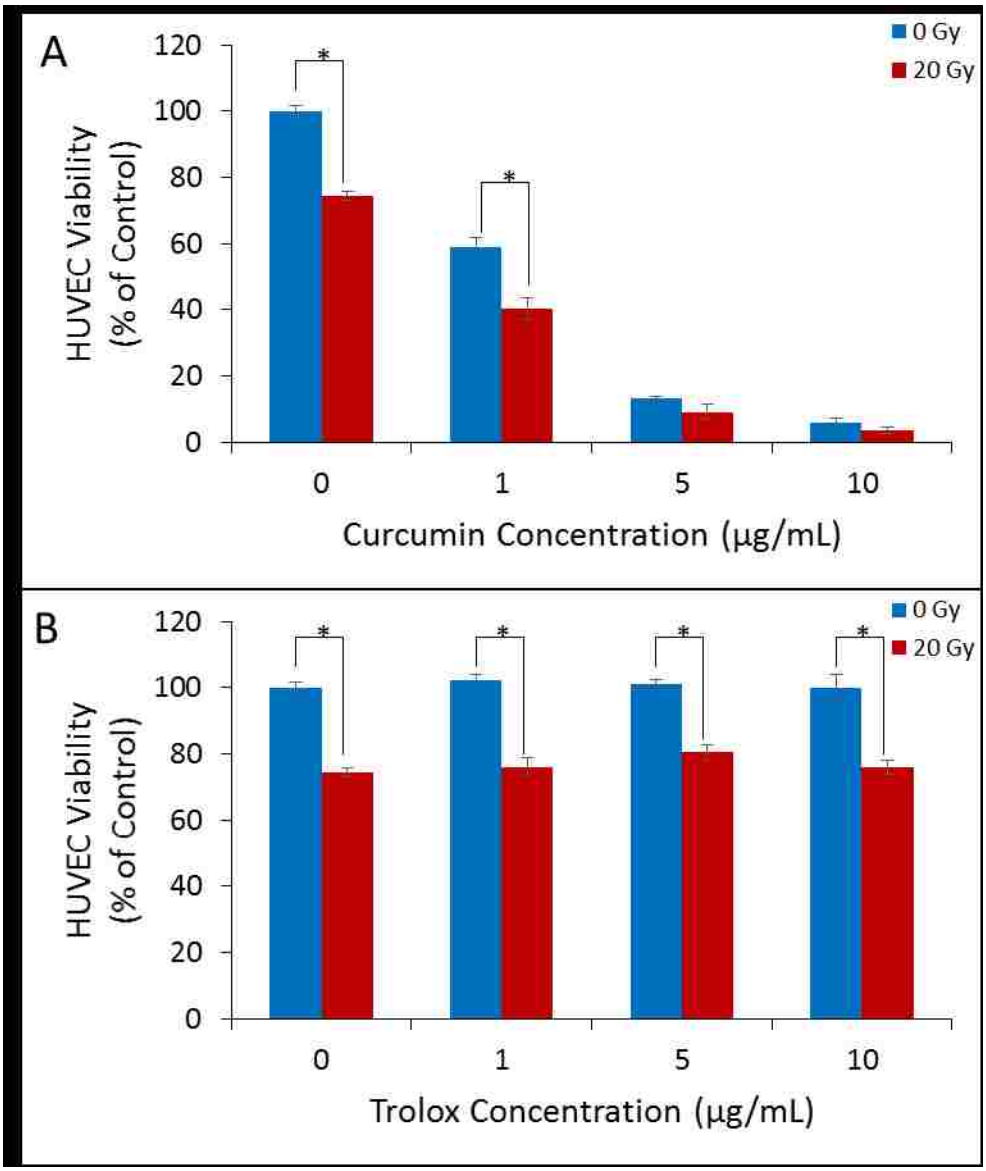

Figure 4-2: HUVEC pretreated with Curcumin/Trolox radiation viability response 72 hours after radiation. Cells seeded at 20,000 cells/cm^2. N=4. Error bars represent standard error. * indicates p-value<0.05 in two-way ANOVA. (A) HUVEC viability as function of curcumin concentration and radiation dose (B) HUVEC viability as function of trolox concentration and radiation dose

4.3.3 Inhibition of ROS generated by radiation

The effect of antioxidants on the irradiated system's ROS generation was measured using DCF-DA. Antioxidant concentrations ranging from 0-10µg/mL were incubated for 1 hour with cells before irradiation. 24 hours after radiation, a DCF fluorescence reading was

performed. Cells treated with only radiation exhibited 124% of control DCF fluorescence. Addition of curcumin to radiated cells reduced this fluorescence to 61%, 14% and 14% of control respectively for 1 μg/mL, 5 μg/mL and 10 μg/mL curcumin treatment. A similar trend was seen with trolox where addition of trolox to radiated cells reduced this fluorescence to 67%, 43% and 35% of control respectively for 1 μg/mL, 5 μg/mL and 10 μg/mL trolox treatment. This indicates that both curcumin and trolox are reducing ROS generated by radiation as expected. DCF-DA assay takes into account background fluorescence from DCF in the media however so it may not accurately portray damage to the individual cells. It should also be noted that the DCF fluorescence is especially low for curcumin at 5 μg/mL and 10 μg/mL concentrations. This is due to cell death from curcumin which halts cellular respiration and ROS generation.

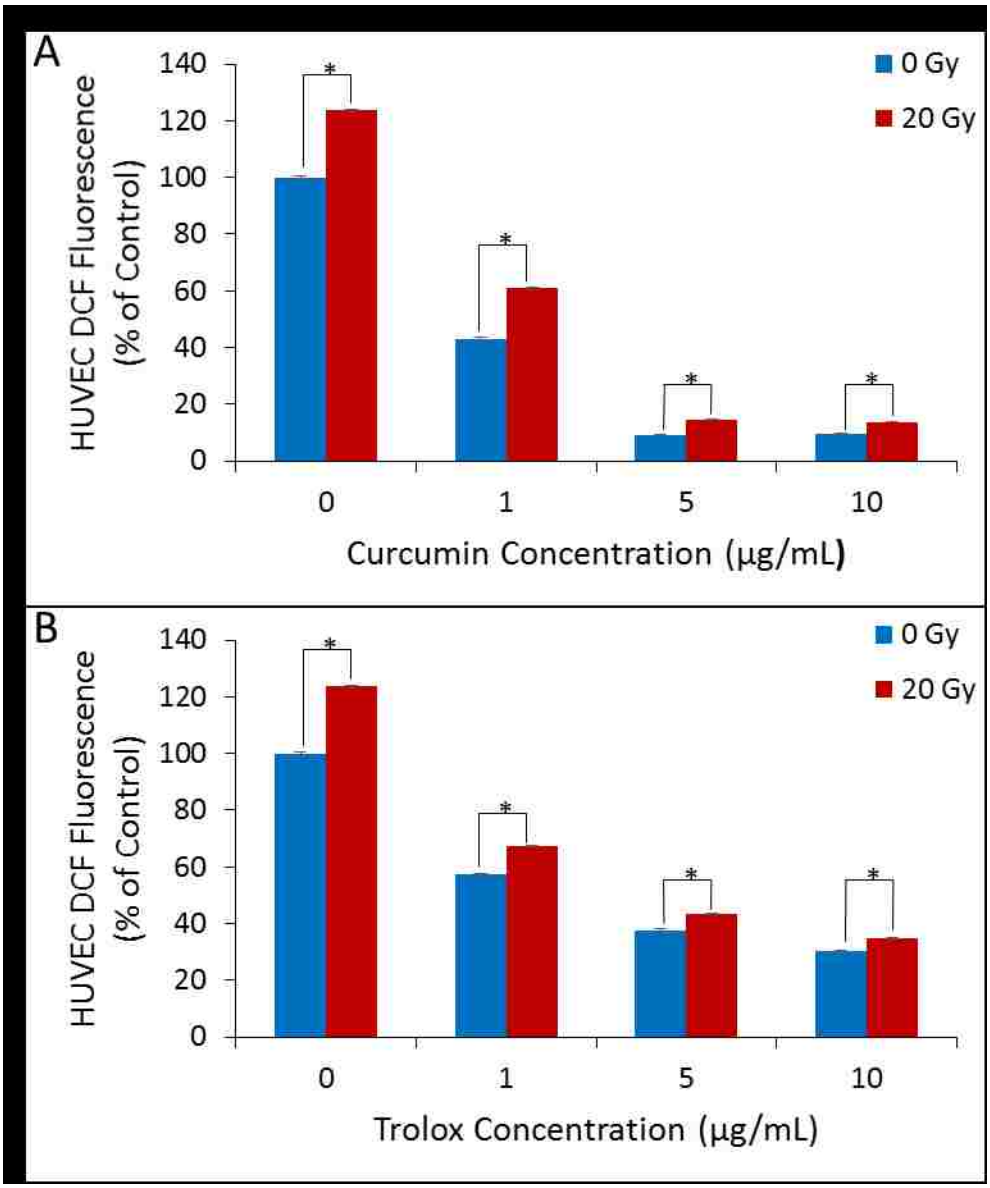

Figure 4-3: HUVEC pretreated with Curcumin/Trolox, radiation DCF fluorescence response 24 hours after radiation. Cells seeded at 20,000 cells/cm^2. N=4. Error bars represent standard error. * indicates p-value<0.05 in two-way ANOVA. (A) HUVEC DCF fluorescence as function of curcumin concentration and radiation dose (B) HUVEC DCF fluorescence as function of trolox concentration and radiation dose

4.3.4 Cell γ-H2AX foci Formation Assay

γ-H2AX foci formation assay was preformed to gauge cellular response and eliminate possible background effects from media. Confluent HUVEC were prepared in chamber slides. One group received no treatments, another received 1µg/mL curcumin treatment, another

received 20 Gy radiation treatment and the last received 1µg/mL curcumin and 20 Gy radiation treatment. The chamber slides were fixed, stained and imaged using fluorescent microscopy. Few cells exhibited γ-H2AX foci formation in groups without radiation treatment. Both the 20 Gy radiation treatment groups exhibited many γ-H2AX foci formations though, indicating severe DNA damage. The cells pretreated with curcumin before radiation had no reduction in γ-H2AX foci formations compared to cells only treated with radiation though. This shows that curcumin has no significant effect on DNA damage in this system. This lack of cellular response to curcumin could also be due to extreme experimental conditions as 20 Gy of radiation completely saturates the cells with activated histones.

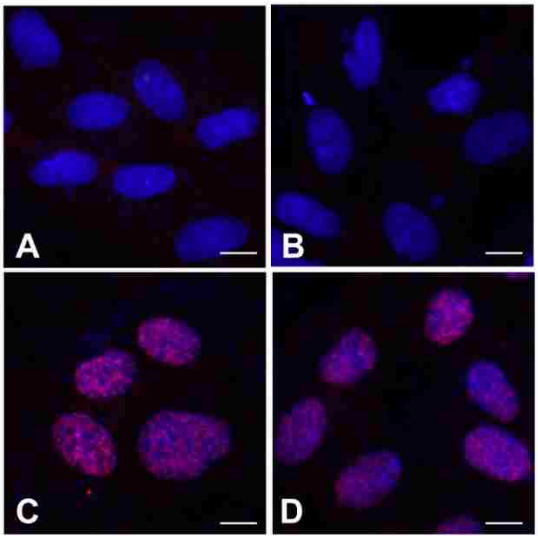

Figure 4-4: HUVEC pretreated with Curcumin, radiation γ-H2AX foci formation response (A) no treatment (B) curcumin treatment (C) radiation treatment (D) curcumin and radiation treatment

4.4 Discussion

The experiments carried out in this chapter were successful in creating a radiation damage model and characterizing curcumin's interaction with radiation in healthy endothelial cells. Curcumin showed reduction in ROS generation in irradiated cells but in a viability assay, curcumin was shown to be toxic to the cells and further reduced the viability of irradiated and

non-irradiated cells alike. Curcumin also showed no measureable effect on the amount of double stand breaks created from radiation dame in radiated cells. This data shows that simply adding antioxidants to an endothelial layer model to reduce ROS does not lead to an increase in viability of cells, as curcumin did not show any protection in radiation damage. This indicates that curcumin's role as a radioprotectant may not be directly a function of its antioxidant capacity and is dependent on factors outside of an endothelial monolayer *in vitro* model. Although this result does not change the conventional thought of how curcumin radioprotects. This data suggests that an endothelial layer does not see much benefit from antioxidant treatment before radiation. Due to all the *in vivo* curcumin radioprotection data in the literature, this would mean curcumin requires a more complex environment to exert a protective effect.

As mentioned previously, the reduction in ROS in the cells seen by curcumin in the DCF assay may be over reported as the media surrounding the HUVEC contributes to fluorescence levels. The radiation dosing of cells may not have been ideal for γ-H2AX foci formation assay as well. It would have been beneficial to use a lower radiation dose so all the cell histones were not saturated. Even if the curcumin was exerting a protective effect, a measureable effect could not be measured at this damage level. A lower dose of 5 Gy may have been better suited than the 20 Gy treatment.

4.5 Conclusions

A radiation damage model was successfully developed using a HUVEC monolayer of cells. The *in vitro* effect of gamma radiation on HUVEC pretreated with curcumin was characterized. Cells treated with curcumin showed significantly less ROS development than both their radiated and non-radiated respective controls. Cells treated with curcumin showed a decrease in viability for both radiated and non-radiated cells. Curcumin pretreatment exhibited

no reduction in γ-H2AX foci formation in cells after radiation damage. These results provide insight into the radioprotective mechanism of curcumin, as the antioxidant capacity has not shown to play a large role in reduction of toxicity or DNA damage to healthy cells in this model.

Chapter 5: Synthesis and Characterization of Curcumin Polymer

5.1 Introduction

Curcumin has been shown to have a low absorption rate, is readily metabolized and quickly excreted from the body [98-101]. A variety of delivery mechanisms have been tested including liposomal curcumin, structural modification of curcumin and curcumin nanoparticles to address these pitfalls and deliver active curcumin to the site of interest. Liposomal curcumin has been shown to have at least equal efficacy in biodistribution as free curcumin[102] and is able to load more curcumin in cells than aqueous-DMSO delivered curcumin[103]. A curcumin analogue, EF-24 was developed and distribution was tested in mice. This molecule had similar activity to curcumin and possessed a longer half-life and lower plasma clearance compared to free curcumin[104]. Cross linked micellar curcumin nanoparticles synthesized with N-isopropylacrylamide, N-vinyl-2-pyrrolidinone and poly(ethyleneglycol) acrylate have been synthesized in a size range below 100 nm and possessed similar efficacy as curcumin *in vivo* and *in vitro* [105]. Each of these methods was able to increase the amount of curcumin delivered when compared to free drug, but better targeting and protection of molecular curcumin is needed.

In order to address this, a Michael addition reaction to form a linear poly(beta-amino ester) (PBAE) was chosen as the method to polymerize curcumin into a functional vehicle for extended release. Poly(beta-amino ester) chemistry employs ester bonds that can be hydrolytically degraded. This incorporation of curcumin into the polymer is promising, as the active curcumin is preserved until release upon the breaking of the ester bond in the polymer. PBAE systems are able to be tuned through choice of acrylates and amines to influence both degree of polymerization and degradation rate as well. Networked polymers can also be

produced though increasing the number of functional groups in the molecules used beyond a 1:1 ratio. Linear PBAE has the advantage that it can be used to develop nanoparticles with targeting antibody coatings.

Curcumin was functionalized into CMA through methods developed by the lab. Primary amines were bought commercially and used for polymerization in order to develop a near linear polymer as the CMA developed is thought to consist mostly of curcumin diacrylate. Through adjustment of reaction conditions a CPBAE polymer can be synthesized and formed into targeted nanoparticles. These particles will be able to degrade, releasing curcumin to exert its therapeutic effect.

5.2 Methods and Materials

5.2.1 Reagents

All solvents were obtained from Sigma-Aldrich or Fisher Scientific. Curcumin was purchased from Chem-Impex International. Acryloyl chloride was purchased from Sigma-Aldrich. All acrylates and amines were purchased from Sigma-Aldrich. PLGA was purchased from DURECT.

5.2.2 Synthesis and characterization of Curcumin Multiacrylate

5.2.2.1 CMA Synthesis Methods

Curcumin Multiacrylate (CMA) was synthesized using protocol developed by our lab in which curcumin is reacted with acryloyl chloride. Briefly, curcumin was dissolved in anhydrous tetrahydrofuran (aTHF) in a three-neck round bottom flask. Triethylamine (TEA) is then added to the solution and the flask is purged with N_2 gas. Acryloyl chloride is added to the solution and the reaction is then allowed to proceed in darkness overnight. To purify the curcumin

multiacrylate product, first TEA-HCl salt is removed using filter paper. THF is then evaporated from the solution using a vacuum pump.

After evaporation, a solid product is recovered. This product is dissolved in anhydrous Dichloromethane (aDCM). In order to remove more TEA in the product, an equal volume of 0.1M HCl was added to this solution, mixed and then centrifuged. The organic phase of CMA+DCM was collected after centrifugation. Next, excess acrylic acid must be removed. An equal volume of 0.1M K_2CO_3 is added to this CMA+DCM solution, mixed and then centrifuged. The organic CMA+DCM phase is collected.

In order to remove residual water $MgSO_4$ is added to the CMA+DCM solution until bubbles are no longer seen escaping. The solution is filtered to remove $MgSO_4$ salt. The CMA+DCM solution placed under a vacuum to remove DCM from the solution. The final CMA product is collected and stored at -80°C.

5.2.2.2 CMA HPLC Characterization

A 1 ml solution of CMA was prepared in acetonitrile at a concentration of 100µg/ml. This sample was run through the HPLC system with a changing gradient methodology. The injection volume was 50 µL. The method begins 50% acetonitrile and 50% aqueous solution. The aqueous solution decreases to 0% over 15 minutes and then remains constant for 5 minutes. The aqueous solution concentration then increases to 50% over 5 minutes. The concentration then remains constant at 50% aqueous for 5 minutes until the method completes at a 30 minute run time. The elution times of material is depicted in a chromatogram at both 210nm and 420nm wavelengths.

5.2.2.3 CMA GPC Characterization

A 1 mL solution of CMA was prepared in THF at a concentration of 5mg/mL. A Shimadzu Providence LC-20 AB HPLC with a refractive index sensor and UV Vis spectrometer with a

Polymer Laboratories 300 x 7.5 mm PLgel 3 µm mixed-E column system was used. This sample was run through the GPC with a 20µL injection volume.

5.2.2.4 CMA Mass Spectrometry

A 1mg/mL solution of CMA in anhydrous acetonitrile was prepared for use in mass spectrometry. A Thermofinnigan mass spectrometer model LTQ with a linear ion trap mass analyzer and electrospray ionization was used to characterize this sample. A spectra was produced in both positive ion and negative ion methodologies.

5.2.2.5 CMA FTIR Characterization

CMA was characterized using Fourier Transformed Infrared spectroscopy. A Varian Digilab stingray FTIR system with a 7000e stepscan spectrometer was used. Solid powder CMA was placed on the crystal and the software methods were used to produce a spectra.

5.2.3 Synthesis and Characterization of Curcumin Poly(beta-amino ester)

5.2.3.1 Adjustment of Amine and Solvent Poly(beta-amino ester)

Preliminary CPBAE synthesis was performed using aDCM and MEK as a solvent for CMA. Trials were performed using 50mg CMA with a 1:1 molar ratio of primary amine. Isobutylamine (IBA), N,N'-Dimethyl- 1,3-propanediamine (NNDA) and methoxypolyethylene glycol amine (MEO) were chosen to test as amine groups. 50 mg of CMA and 100µL of solvent were added into each vial and vortexed. The appropriate amine was then added under the hood and stirred at 60°C for 24 hours. Reactions were then solubilized in THF and characterized using GPC.

5.2.3.2 Precipitation of Curcumin Poly(beta-amino ester)

CPBAE was synthesized at a 1:1.5 molar ratio of CMA to IBA. CMA was solubilized in MEK at a concentration of 500mg/mL. IBA was added and the CMA-MEK solution and the reaction was heated to 60°C, stirred and left to react for 24 hours. The polymer was collected

and dissolved in THF. The THF-CPBAE solution is then added into cold ethanol at a 1:10 THF:ethanol volume ratio. The solution is then centrifuged at 4500 rpm at 4°C for 1 hour. The supernatant is decanted and the CPBAE solid is freeze dried. GPC was used to determine the molecular weight of the polymer and its size distribution compared to CPBAE without precipitation.

5.2.3.3 Adjustment of Molar Ratios of Acrylate to Amine

Curcumin PBAE was produced at varying ratios of acrylate to amine in triplicate. With the assumption that CMA is 100% curcumin diacrylate, a range of reactions including 1:0.5, 1:1, 1:1.5 and 1:2 molar ratio of CMA to IBA were produced. 50 mg of previously synthesized CMA was weighed into a glass vial. 100 µL of MEK was then added to each vial and vortexed until fully dissolved. The appropriate molar ratio of IBA was then added into each vial. A stir bar was then added to each vial, capped and then heated to 60°C and stirred for 24 hours. GPC was used to determine the molecular weight of the polymers.

5.2.3.4 Adjustment of Acrylate and Reaction Rate Conditions Poly(beta-amino ester)

Polymers were prepared in similar conditions to previous methods of CPBAE synthesis with added variables to influence reaction rate. These being the addition of 1,8-Diazabicyclo[5.4.0]undec-7-ene (DBU) catalyst and increased temperature of 90°C compared to 60°C. As well as adjusting reaction rate variables, acrylates including CMA, Polyethylene(glycol) diacrylate (PEGDA), Diethylene(glycol) diacrylate (DEGDA) and 1,6-Hexanediol diacrylate (HEXDA) were tested.

Briefly, reagents were added into a vial with a stir bar and placed into an oil bath at 60°C or 90°C. Each vial contained a total mass of 200 mg with a 1:1 acrylate to amine ratio. No extra solvent was added to reactions except for CMA groups which were solvated with MEK. DBU

catalyst was added at 50 mol% of amine used. Reactions were left to proceed for 24 hours with stirring.

The product was then suspended in THF after 24 hours of stirring. A sample at a concentration of approximately 10 mg/ml was prepared and analyzed in the hydrophobic GPC column.

5.2.3.5 SEM imaging Curcumin Poly(beta-amino ester)

Curcumin poly(beta-amino ester) was synthesized at a molar ratio of 1:1.5 CMA:IBA and purified by precipitation in ethanol. CPBAE was suspended in acetone and placed on an SEM stub. The stub was left open to atmosphere to evaporate off the acetone. A Hitachi S-4300 with cold cathode field emission was used to produce images of the CPBAE.

5.2.3.6 Solvent Cast Curcumin Poly(beta-amino ester) Films

1:1.5 CPBAE and 50,000 MW PLGA were both dissolved in DCM at a concentration of 1 mg/mL. CPBAE solution and PLGA solution were mixed to various ratios of CPBAE to PLGA. The weight percent PLGA in the polymer was increased from 0 to 100 in increments of 20. Using a pipette, solutions were spread into films on glass slides and were left to evaporate overnight.

5.2.3.7 Differential Scanning Calorimetry Curcumin Poly(beta-amino ester)

Differential Scanning Calorimetry (DSC) was performed on solvent cast CPBAE-PLGA polymer films from 0wt% PLGA to 100wt% PLGA in increments of 20wt%. The method used preheated the sample to 55° C and cooled to -10°C in order to give all samples similar heating history before running the test. Heat flow was then characterized from -10° C to 150° C. The glass transition point was characterized as the minimum of the trough when the sample was heated.

5.2.3.8 FTIR Curcumin Poly(beta-amino ester)

CPBAE was characterized using Fourier Transformed Infrared spectroscopy. A Varian Digilab stingray FTIR system with a 7000e stepscan spectrometer was used. Solid powder CPBAE was placed on the crystal and the software method was used to create a spectra.

5.2.4 Curcumin Poly(beta-amino ester) Nanoparticle Synthesis

5.2.4.1 Nanoparticle Synthesis Methods

Nanoparticles were synthesized using a nanoprecipitation method. Both CPBAE and PLGA polymer were dissolved in acetone at a concentration of 5mg/mL. Experimental groups of pure CPBAE, pure PLGA and 30:70 wt% CPBAE:PLGA were chosen. 1 mL of the organic solution was added dropwise into 4 mL of DI while vortexing at 2000 rpm. Acetone was then removed from the suspension under a vacuum pump.

5.2.4.2 Dynamic Light Scattering (DLS) Size Characterization

PLGA nanoparticles, CPBAE nanoparticles and 30:70 CPBAE:PLGA nanoparticles at a concentration of 1mg/mL in DI water were put into a cuvette. A Malvern Zetasizer Nano DLS was used to measure nanoparticle size.

5.2.4.3 Nanoparticle Zeta Potential Characterization

PLGA nanoparticles, CPBAE nanoparticles and 30:70 CPBAE:PLGA nanoparticles at a concentration of 1mg/mL in DI water were put into a cuvette. A Malvern Zetasizer Nano DLS was used to measure nanoparticle zeta potential.

5.2.4.4 DLS Size Characterization of Nanoparticles Over Time

30:70 CPBAE:PLGA nanoparticles at 1mg/ml concentration in DI water were prepared. A Malvern Zetasizer Nano DLS was used to measure nanoparticle size over time in 15 minute intervals. The chamber was kept at a constant 25°C.

5.2.4.5 SEM Imaging of Nanoparticles

30:70 wt% CPBAE:PLGA nanoparticles were synthesized using previous methods. Nanoparticles were suspended in acetone and placed on an SEM stub. The solution was left to evaporate of the acetone. A Hitachi S-4300 with cold cathode field emission was used to produce images of the particles.

5.2.5 Release of Curcumin from Curcumin Poly(beta-amino ester)

5.2.5.1 Solid Polymer Curcumin Release UV-Vis

Freeze dried CPBAE solid was crushed and weighed to 50 mg of theoretical curcumin (74.5 mg CPBAE). The CPBAE was then added to 1 L of 0.1 wt% SDS PBS. This was stirred continuously at 37˚C and samples were taken at given time points. The samples were centrifuged at 10,000 rpm for 5 minutes. The supernatant was saved and measured in the UV-Vis compared to a calibration curve of free curcumin at 420nm wavelength.

5.2.5.2 Nanoparticle Curcumin Release UV-Vis

Freeze dried CPBAE dissolved in acetone was added into 0.1wt% SDS in PBS. The final concentration of the solution was 74.5ug/ml cPBAE in 1wt% SDS in PBS (50 µg of theoretical curcumin). The stock solution was divided into 1 mL aliquots and each was placed in the agitating incubator at 37°C. Vials were taken off at given time points and then centrifuged at 10,000 rpm for 5 minutes. The supernatant was saved and measured in the UV-Vis compared to a calibration curve of free curcumin at 420nm wavelength.

5.2.5.3 Nanoparticle Curcumin Release HPLC

Pure CPBAE dissolved in acetone was added into 1wt% SDS in PBS. The final concentration of the solution was 74.5ug/ml CPBAE in 0.1wt% SDS in PBS (50 µg of theoretical curcumin). The stock solution was divided into 1 mL aliquots and each was placed in the

agitating incubator. Vials were taken off at given time points and then centrifuged at 10,000 rpm for 5 minutes. Measured curcumin standards were prepared in ACN and used as a calibration curve to determine the amount of curcumin in each supernatant.

5.2.5.4 Nanoparticle Curcumin Release GPC

Pure CPBAE dissolved in acetone was added into 0.1wt% SDS in PBS. The final concentration of the solution was 74.5ug/ml CPBAE in 0.1wt% SDS in PBS (50 µg of theoretical curcumin). The stock solution was divided into 1 mL aliquots and each was placed in the agitating incubator. Vials were taken off at given time points and then centrifuged at 10,000 rpm for 5 minutes. GPC was used to measure molecular weight of degraded CPBAE precipitate over time.

With the similar conditions, CPBAE polymer was solubilized in acetone and then added into 0.1wt% SDS PBS for nanoparticle degradation trials. Samples were taken at time points and the entire solution was freeze dried. The solid recovered after freeze drying was dissolved in THF and characterized through GPC. GPC UV-Vis chromatograms at 420nm were developed for each time point. UV-Vis at 420nm was used to capture a chromatograph of curcuminoids as a function of elution time.

5.3 Results

5.3.1 Synthesis and Characterization of Curcumin Multiacrylate

5.3.1.1 HPLC Characterization of CMA

Curcumin Multiacrylate was synthesized and characterized using HPLC. The characteristic peak of curcumin at 8 minutes was not seen, indicating that the product only acrylated curcumin. As shown in the chromatogram (UV detector set at 420nm), a major peak was observed at 13 minutes elution time as well as two smaller peaks at 11.5 and 12 minutes. In

a second chromatogram (UV detector set at 210m), peaks were observed at 10.8, 11.5, 12 and 13 minutes. On the HPLC chromatogram set at 420nm, the 13 minute peak is thought to be curcumin diacrylate while 11.5 and 12 minutes are thought to be curcumin monoacrylate or curcumin triacrylate.

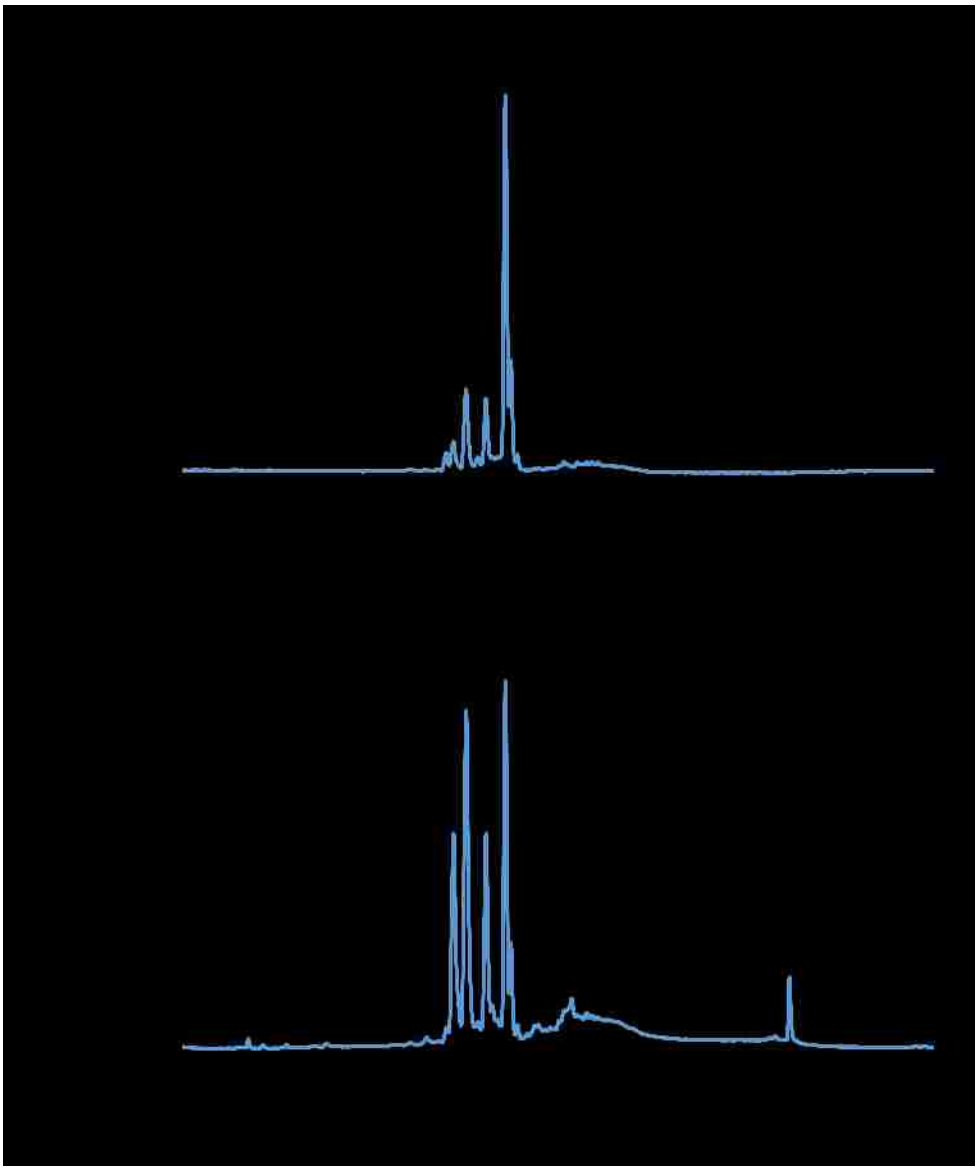

Figure 5-1: HPLC chromatogram CMA(A) 420nm HPLC chromatogram 100µg/mL CMA in acetonitrile (B) 210nm HPLC chromatogram 100µg/mL CMA in acetonitrile

5.3.1.2 GPC Characterization of CMA

Curcumin Multiacrylate was synthesized and characterized using GPC. When the IR chromatogram is examined, a major peak is seen at 21 minutes elution corresponding to low molecular weight species below 500 molecular weight. This peak corresponds to free CMA species. A significant peak from 16 minutes to 20 minutes is also observed, this corresponds to species between 1000 and 10000 Mw. This indicates that CMA is not pure and has some side reaction product. A GPC chromatogram (UV detector set to 420m) shows that curcuminoids are present in the 16-20 minute elution peak as well as the expected 21 minute elution peak where CMA would be expected. This shows that significant CMA is polymerized or aggregated and is not accessible.

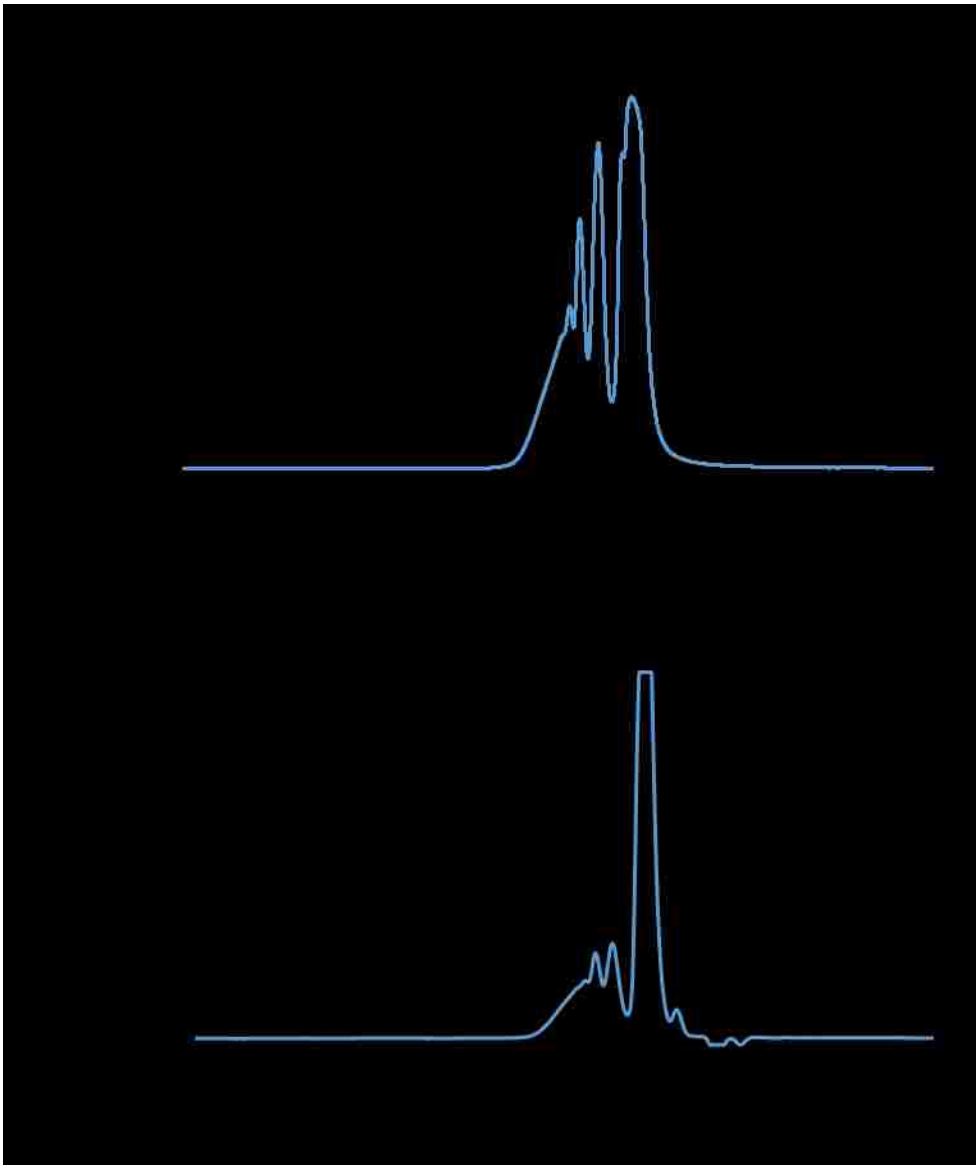

Figure 5-2: GPC chromatogram CMA (A) 420nm GPC chromatogram 5mg/mL CMA in THF (B) IR GPC chromatogram 5mg/mL CMA in THF

5.3.1.3 Mass Spectrometry Characterization of CMA

CMA was characterized using both negative ion and positive ion mass spectrometry. Positive ion spectra indicates strong peaks at 477 and 531 molecular weight. These peaks correspond to curcumin diacrylate and curcumin triacrylate respectively. Other peaks are observed in the lower spectrum as well as higher in the spectrum indicating multiple impurities in the CMA. Negative ion spectra indicates a very strong peak at 475 which corresponds to

curcumin diacrylate. Other species are observed above and below curcumin diacrylate but are much lower in relative abundance.

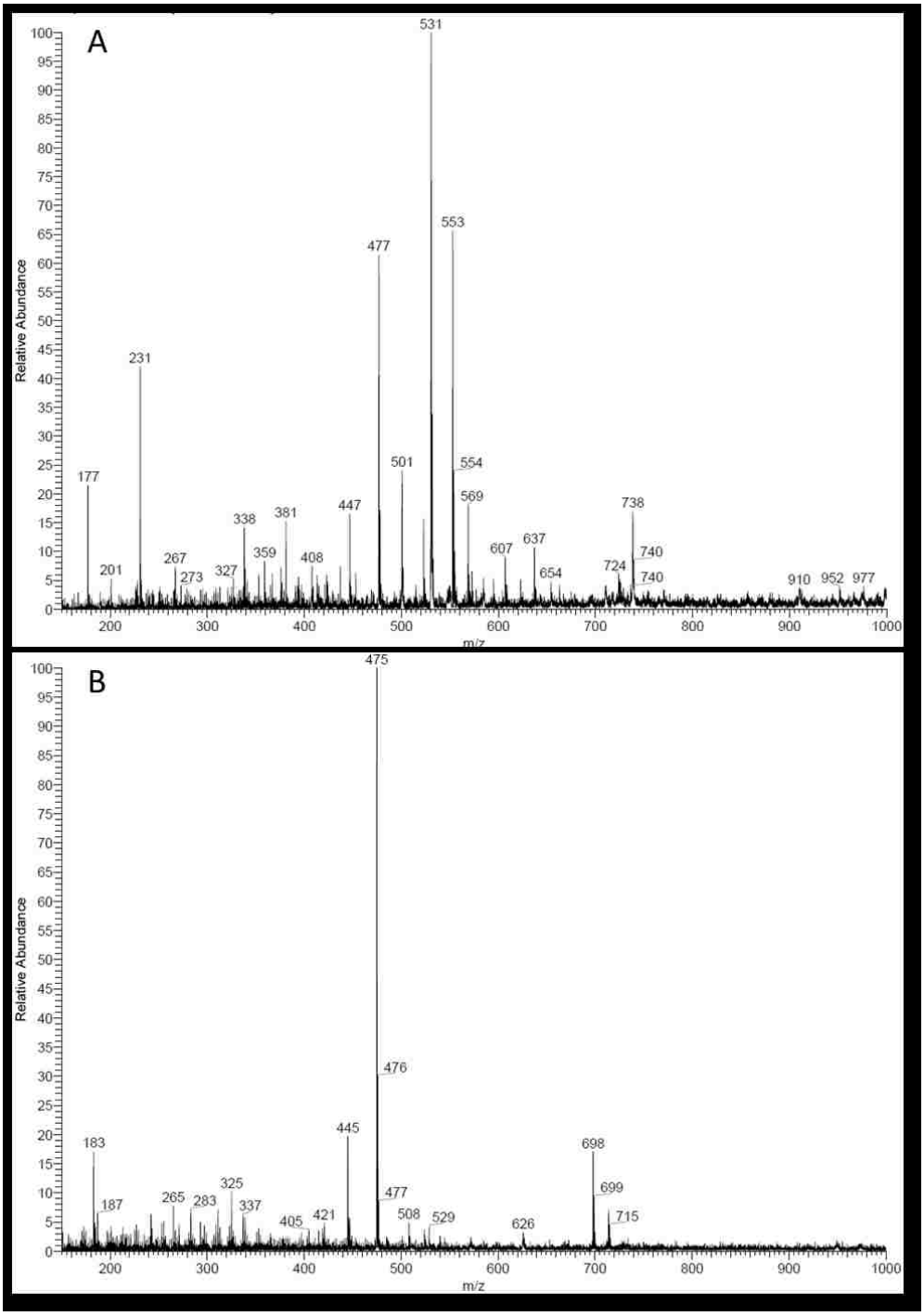

Figure 5-3:Mass spectrometry spectra CMA (A) Mass Spectrometry CMA Positive Ion Spectra (B) Mass Spectrometry CMA Negative Ion Spectra

5.3.1.4 CMA FTIR Characterization

CMA was characterized using FTIR. Significant points of interest are the 2800-3000 range which indicates carboxylic acid and the 3500 sharp peak which represents a phenol group. There was no sharp peak observed at 3500, which indicates that the CMA did not have an abundance of phenol groups as would be expected in curcumin. Carboxylic acid groups should be present in the CMA and a weak peak is seen in the 2800-3000 range indicating such.

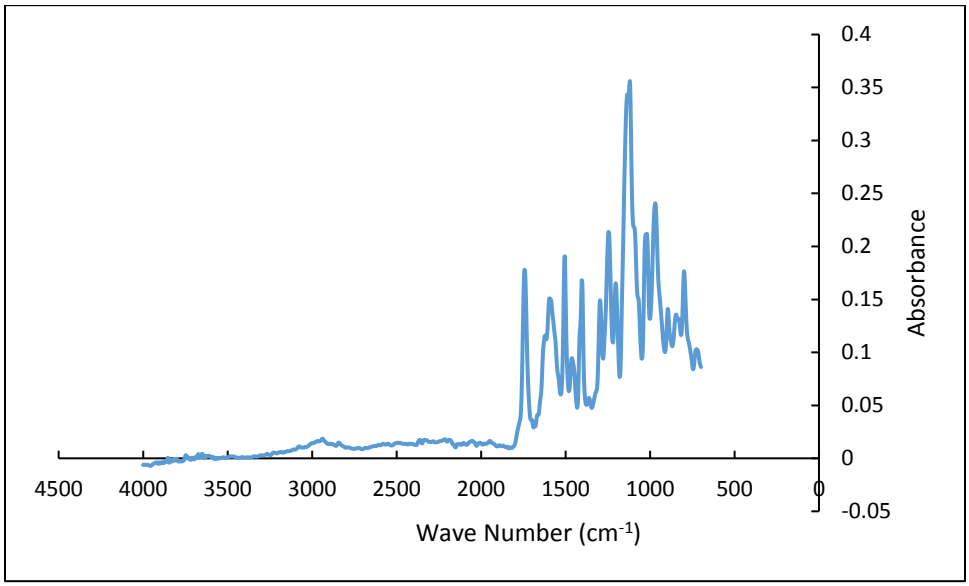

Figure 5-4: CMA FTIR spectrogram

5.3.2 Curcumin Poly(beta-amino ester) Synthesis

5.3.2.1 Adjustment of Amine Poly(beta-amino ester)

CPBAE reactions were collected and prepared for GPC characterization. Both MEK and DCM solvents for the CMA-IBA reactions produced polymer at a molecular weight of 2850 and 2900 molecular weight respectively. The Reactions using NNDA and MEO all became crystalline solids and would not dissolve in THF or ACN. These did not produce polymer and could not be characterized using GPC. Based off of these results IBA was used as the primary amine in further polymerization experiments.

Table 5-1: Molecular weight of CPBAE as a function of reaction conditions

	IBA	NNDA	MEO
MEK	2850	No signal	No signal
DCM	2900	No signal	No signal

5.3.2.2 Precipitation of Curcumin Poly(beta-amino ester)

GPC results showed that 1:1.5 CMA:IBA CPBAE that was not precipitated has a molecular weight of 2500 and a PDI of 5.7. Single precipitation in ethanol was found to have a molecular weight of 6600 with a PDI of 2.0. This change in molecular weight from precipitation can be seen in the change in the polymer's low molecular weight fraction peak past 20 minutes in both UV-Vis and IR spectrograms from GPC. In the un-precipitated polymers (A) and (C) strong peaks are observed in the polymer's low molecular weight fraction peak past 20 minutes. After the polymer was precipitated in ethanol, (B) and (D) weaker peaks were observed in the polymers low molecular weight elution time past 20 minutes.

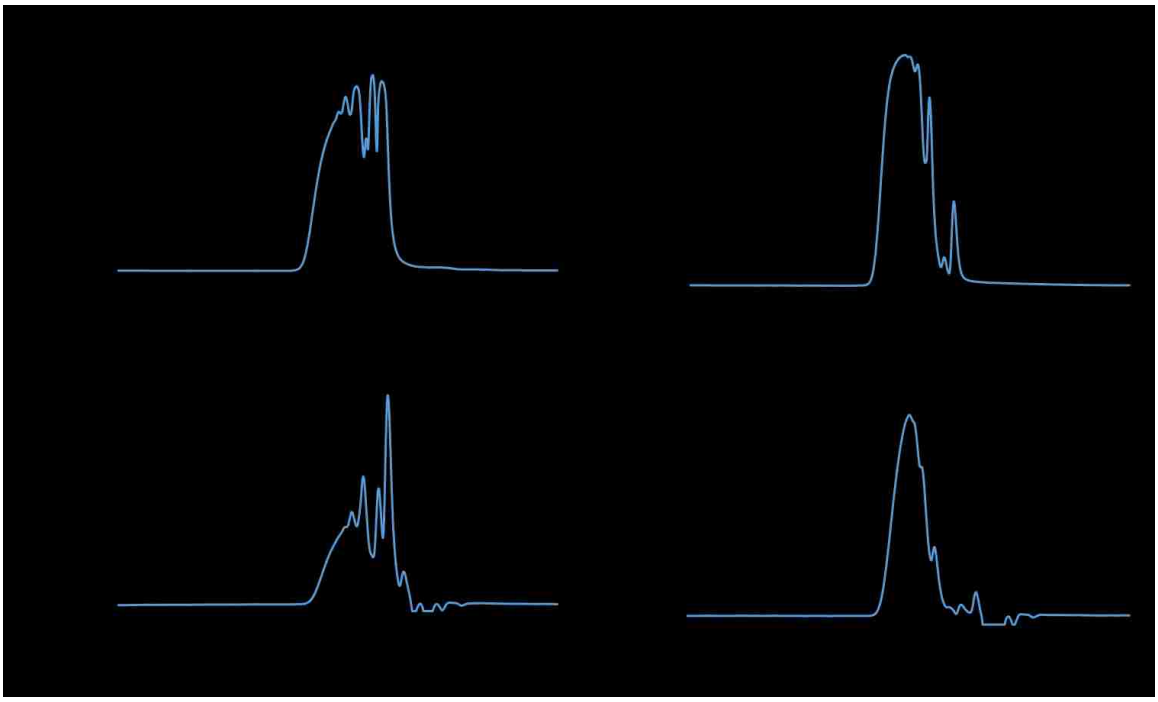

Figure 5-5: CPBAE IR and 420nm UV Vis chromatogram(A) GPC 420 nm UV Vis Chromatogram 1:1.5 CPBAE unprecipitated (B) GPC 420nm UV Vis Chromatogram 1:1.5 CPBAE precipitated (C) GPC IR Chromatogram 1:1.5 CPBAE unprecipitated (D) Figure: GPC IR Chromatogram 1:1.5 CPBAE precipitated

5.3.2.3 Adjustment of Molar Ratios of Acrylate to Amine

GPC results showed that molecular weight of the resulting polymer increased as the molar ratio of IBA increased up to 1:1.5 and then began to decrease as the ratio increased to 1:2. These ratios were calculated assuming that 100% of the CMA is diacrylate and as this is not the case as shown by previous data. This theoretical 1:1.5 ratio has a relative maximum polymerization so was chosen for further testing of the polymer.

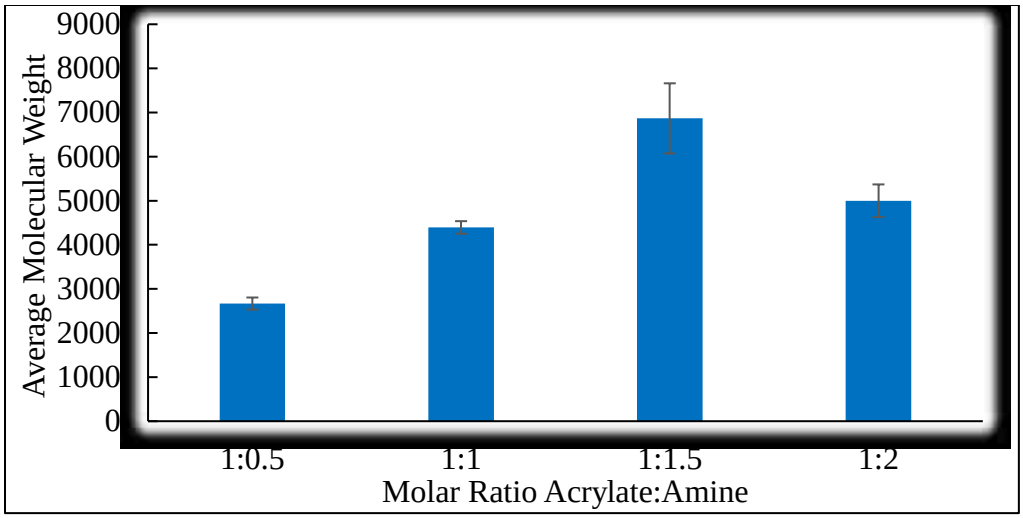

Figure 5-6: GPC assessment of CPBAE average molecular weight

5.3.2.4 Adjustment of Acrylate and Reaction Conditions Poly(beta-amino ester)

IBA was found to be the only primary amine capable of polymerizing with CMA in previous polymerization reactions. Based off of this, multiple acrylates including CMA, HEXDA, DEGDA and PEGDA were all reacted with IBA at different reaction conditions including temperature change and addition of catalyst. This was done in hopes to see if copolymer formation with CMA and another acrylate could be produced at a later point. CMA-IBA polymer showed similar GPC results at both 60°C and 90°C reaction conditions with polymerization with a molecular weight of 6000. The addition of DBU catalyst caused the reaction product to be fully crystalline and no GPC results could be gathered. PEGDA-IBA was unable to form polymer under any temperature or catalyst condition. This may be due to PEGDA being hydrophilic and IBA being hydrophobic. HEXDA and DEGDA both had mixed results concerning polymerization with IBA. Lower temperature at 60°C produced no polymerization. HEXDA polymerized with IBA at 90°C and the GPC molecular weight was 1400. HEXDA polymerized with IBA to an even greater extent with the addition of DBU as the GPC molecular weight was 4000. DEGDA-IBA polymerization followed a similar pattern where DEGDA polymerized with IBA at 90°C and the

GPC molecular weight was 2000. DEGDA polymerized with IBA to an even greater extent with the addition of DBU as the GPC molecular weight was 4000.

Table 5-2: CPBAE molecular weight as a function of reaction conditions

	CMA	HEXDA	DEGDA	PEGDA
60°C	6000	No signal	No signal	No signal
90°C	6000	1400	2000	No signal
60°C + DBU	No signal	No signal	No signal	No signal
90°C + DBU	No signal	4000	4000	No signal

5.3.2.5 SEM imaging Curcumin Poly(beta-amino ester)

SEM images were taken of the polymer film. From the SEM image it can be seen that the polymer is brittle as many cracks are seen after the solvent evaporation process.

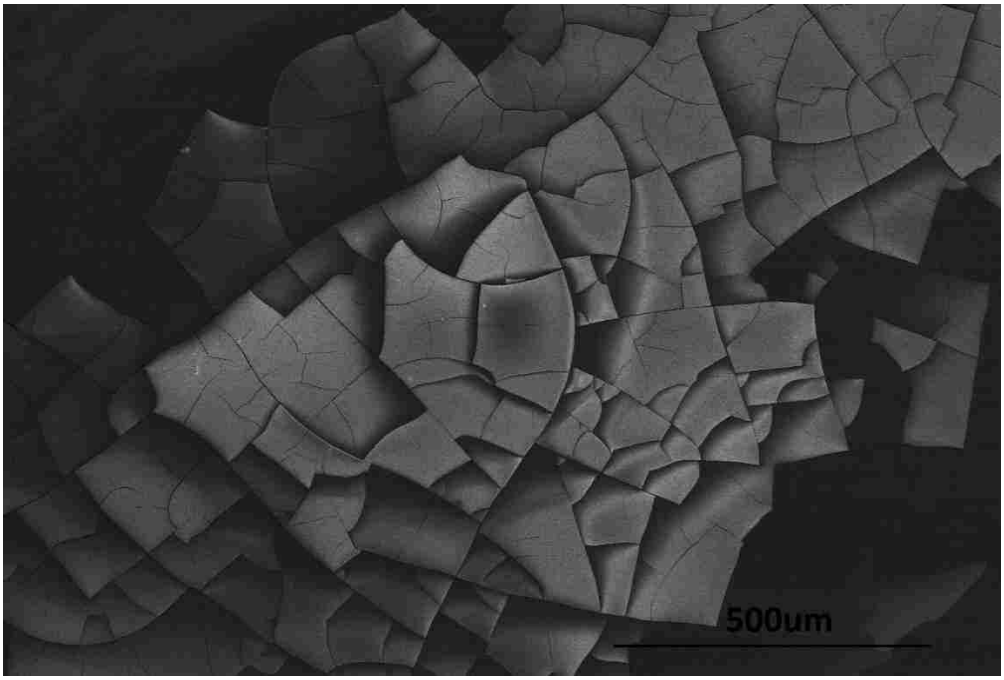

Figure 5-7: SEM image of Curcumin Poly(beta-amino ester) polymer

5.3.2.6 Solvent Cast Curcumin Poly(beta-amino ester) films

CPBAE-PLGA polymer films were synthesized using precipitated 1:1.5 CPBAE and 50,000 molecular weight PLGA. The weight percent PLGA in the polymer was increased from 0 to 100 in increments of 20. After the films were evaporated phase separation between CPBAE and PLGA was observed in the 40wt% PLGA group and to a lesser extent in the 20wt% PLGA group. 0wt% PLGA, 20wt% PLGA and 40wt% fractured upon mechanical stimulation. 60wt% PLGA, 80wt% PLGA and 100wt% PLGA were more pliable and less prone to brittle fracture upon mechanical stimulation.

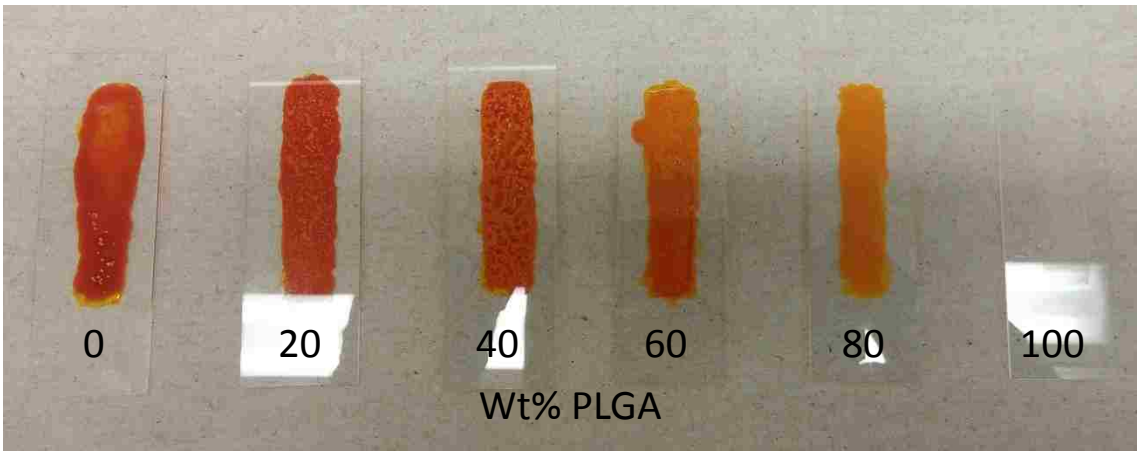

Figure 5-8: Solvent cast PLGA:CPBAE films in DCM

5.3.2.7 Differential Scanning Calorimetry Curcumin Poly(beta-amino ester)

Differential Scanning Calorimetry was performed on solvent cast CPBAE-PLGA polymer films from 0wt% PLGA to 100wt% PLGA in increments of 20wt%. The glass transition temperature was found to be highest with 0wt% PLGA at 68°C. As the percentage of PLGA in the polymer was increased the glass transition temperature decreased to a minimum of 33°C at 100wt% PLGA. This data correlates to observations of the macroscopic films and their brittle

behavior. If CPBAE were to be molded or extruded, it will be necessary that it has a lower glass transition point. Addition of PLGA at 40wt% or 60wt% may be necessary to achieve this end.

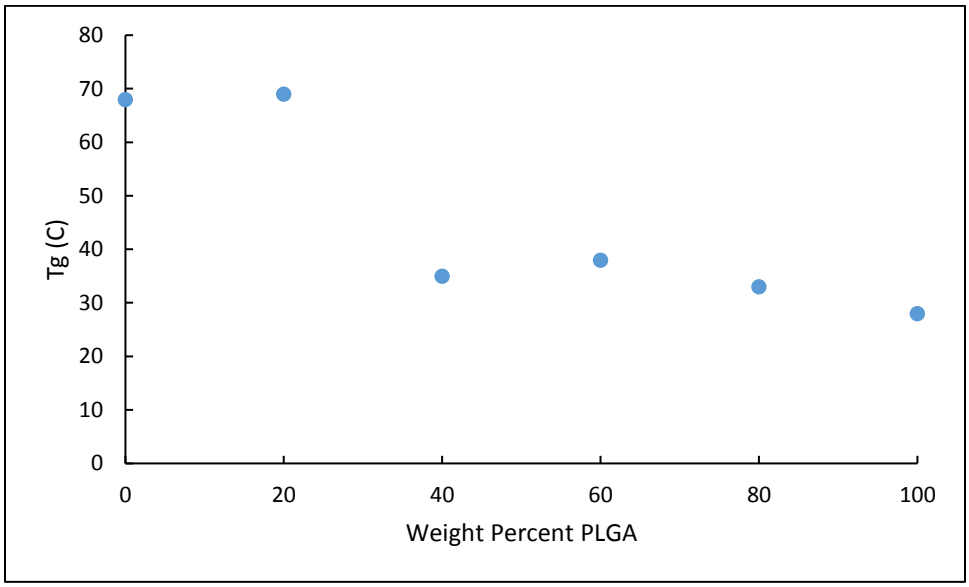

Figure 5-9: Glass transition temperature as a function of CPBAE content

5.3.2.8 FTIR Curcumin Poly(beta-amino ester)

Significant points of interest are the 2800-3000 range which indicates carboxylic acid, the 3300-3500 range which represents amine groups and the 3500 sharp peak which represents a phenol group. Carboxylic acid and amine groups are present in the CPBAE. The best indicator for polymerization however would be C-N bonds which are characteristic at 1000-1250. This is obscured by other peaks and is hard to distinguish however. There was no sharp peak observed at 3500, which shows that the CMA did not have and phenol groups like the curcumin.

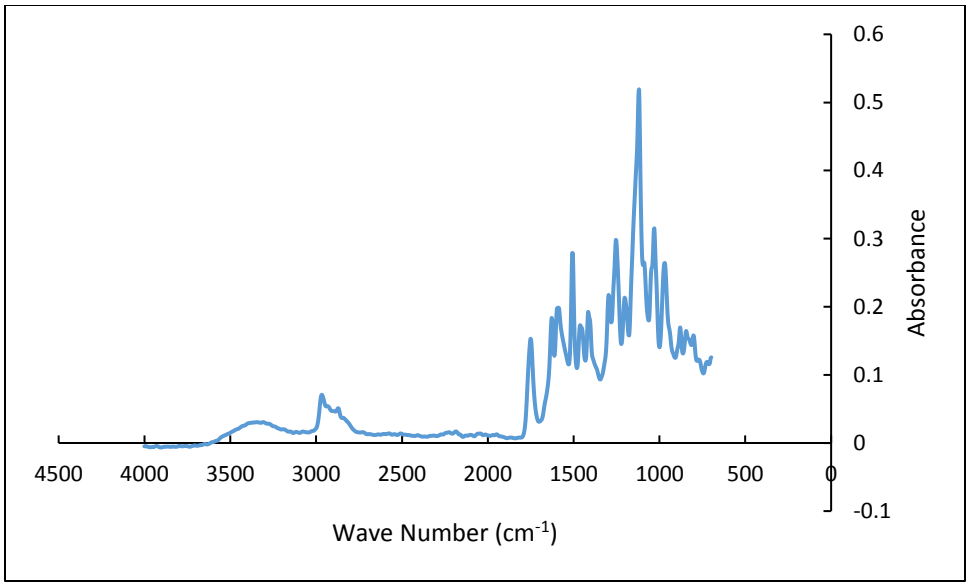

Figure 5-10: Curcumin Poly(beta-amino ester) FTIR spectrogram

5.3.3 Curcumin Poly(beta-amino ester) Nanoparticle Synthesis

5.3.3.1 Dynamic Light Scattering (DLS) Size Characterization

PLGA nanoparticles, CPBAE nanoparticles and 30:70 CPBAE:PLGA nanoparticles were prepared using nanoprecipitation. PLGA nanoparticles were found to have a Z-average diameter of 70.8 +/- 1.7 nm and a PDI of 0.031 +/- 0.022. CPBAE nanoparticles had a Z-average diameter of 92.5 +/-19.5 nm and a PDI of 0.026 +/- 0.011. 30:70 CPBAE:PLGA blended nanoparticles had a Z-average diameter of 86.5 +/- 6.3 nm and a PDI of 0.015 +/- 0.013. This nanoparticle size is ideal for drug delivery as particles above 200 nm are not effective in intravenous delivery. The stability of the particles was tested for the same groups using zeta potential. The zeta potential was observed to be -30.2 +/- 2.3 mV, -20.3 +/- 3.6 mV and -28.1 +/- 1.8 mV for PLGA nanoparticles, CPBAE nanoparticles and 30:70 CPBAE:PLGA nanoparticles respectively. A nanoparticle suspension with zeta potential with absolute value 60 mV has excellent stability. An absolute value of 30 mV has moderate stability and 0 mV is prone to rapid aggregation. The stability of the 30:70 nanoparticles in DI water was tested further tested as the zeta potential

did not indicate strong stability. The particles started at a Z-average diameter of 97 nm and plateaued at approximately 120 nm by 10 hours. This indicates that the particles are relatively stable and remain under 200 nm in size.

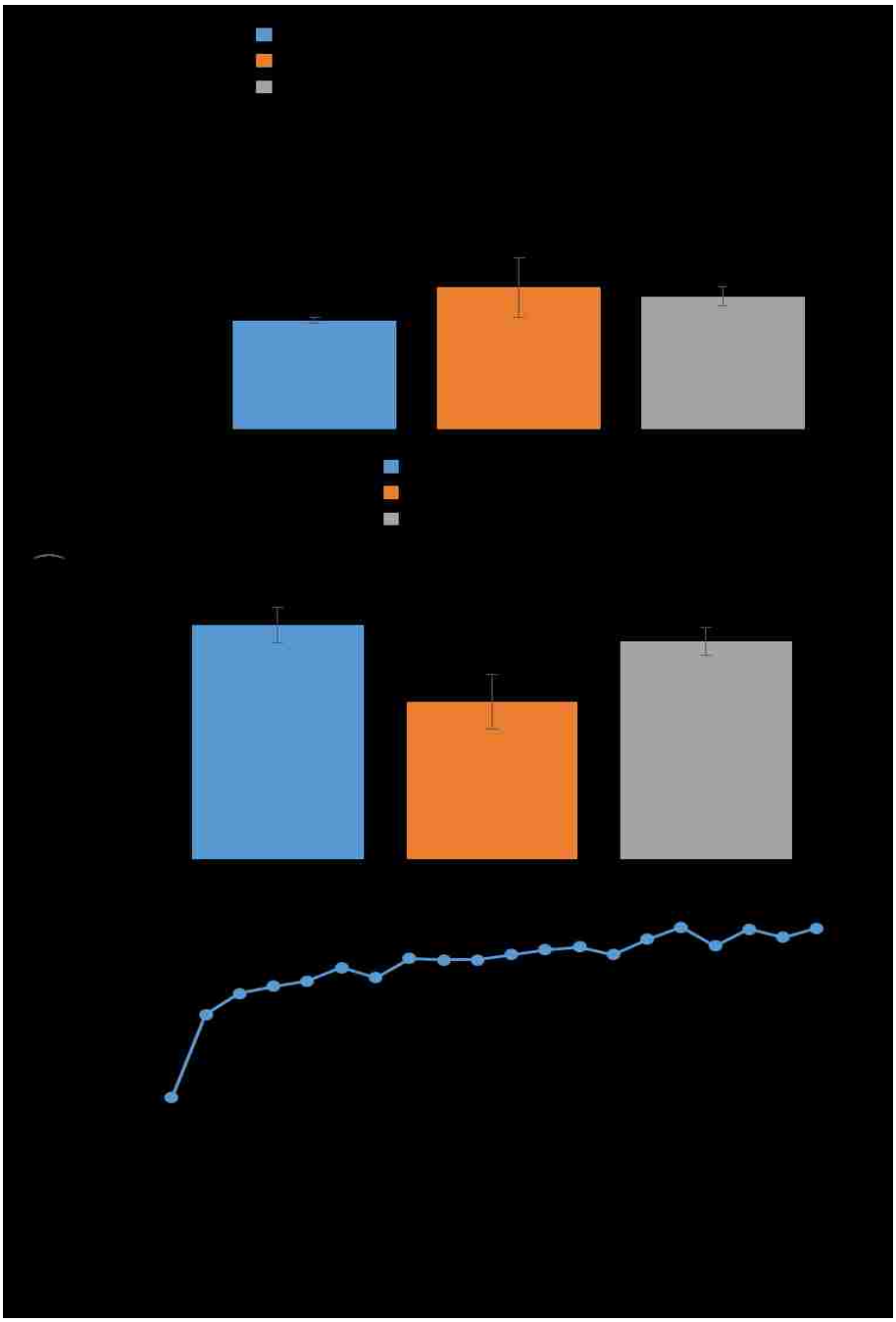

Figure 5-11: Characterization of CPBAE nanoparticle size and shape (A) DLS size characterization of nanoparticles (B) Zeta potential characterization of nanoparticles (C) DLS size characterization of 30:70 CPBAE:PLGA nanoparticles over time

5.3.3.2 SEM Imaging of Nanoparticles

SEM images of 30:70 CPBAE:PLGA nanoparticles were taken to further examine the size distribution and morphology of the particles. SEM images show that the particles are approximately 120 nm which is in line with DLS data gathered. The particles take the form of dented spheres which is unusual. This may be due to CPBAE and PLGA being of different molecular weights and structures, creating imperfect spheres when mixed.

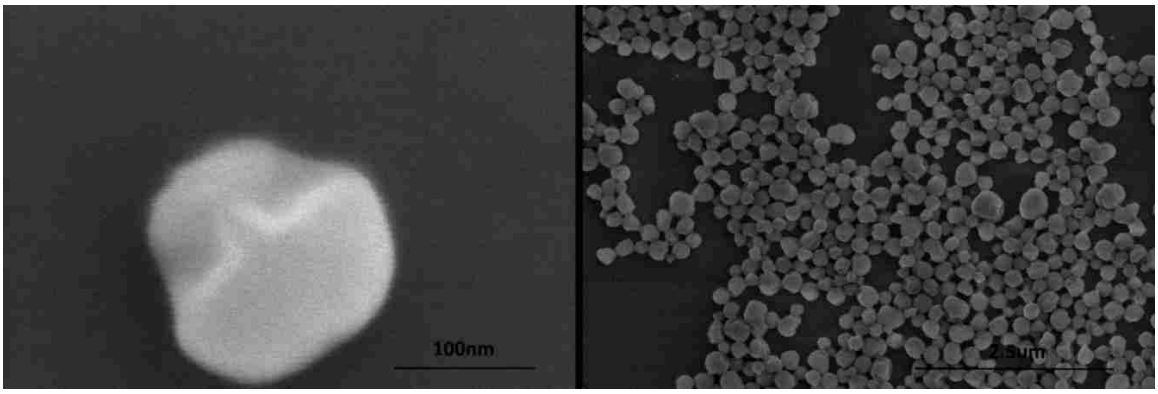

Figure 5-12: SEM image 30:70 CPBAE:PLGA Nanoparticles

5.3.4 Release of Curcumin from Curcumin Poly(beta-amino ester)

5.3.4.1 UV Vis characterization of Curcumin Release

CPBAE polymer was solubilized in acetone and then added into 0.1wt% SDS PBS for nanoparticle degradation trials. Solid CPBAE was added into 0.1wt% SDS PBS directly for the solid polymer degradation trial. Both experiments measured the curcumin release through UV Vis. Curcumin nanoparticles had a high initial burst release of curcumin where 5% of the total load was released by the first time point. The solid polymer exhibited no release of curcumin for 5 days. This is most likely due to polymer swelling with water before it could hydrolytically

degrade. Although the initial release pattern differs, both systems have a maximum release of theoretical curcumin at approximately 20%. This indicates that the theoretical maximum curcumin is not correct. This could be due to CMA not being ideal, side reactions creating non-ideal CPBAE polymer or a combination of both.

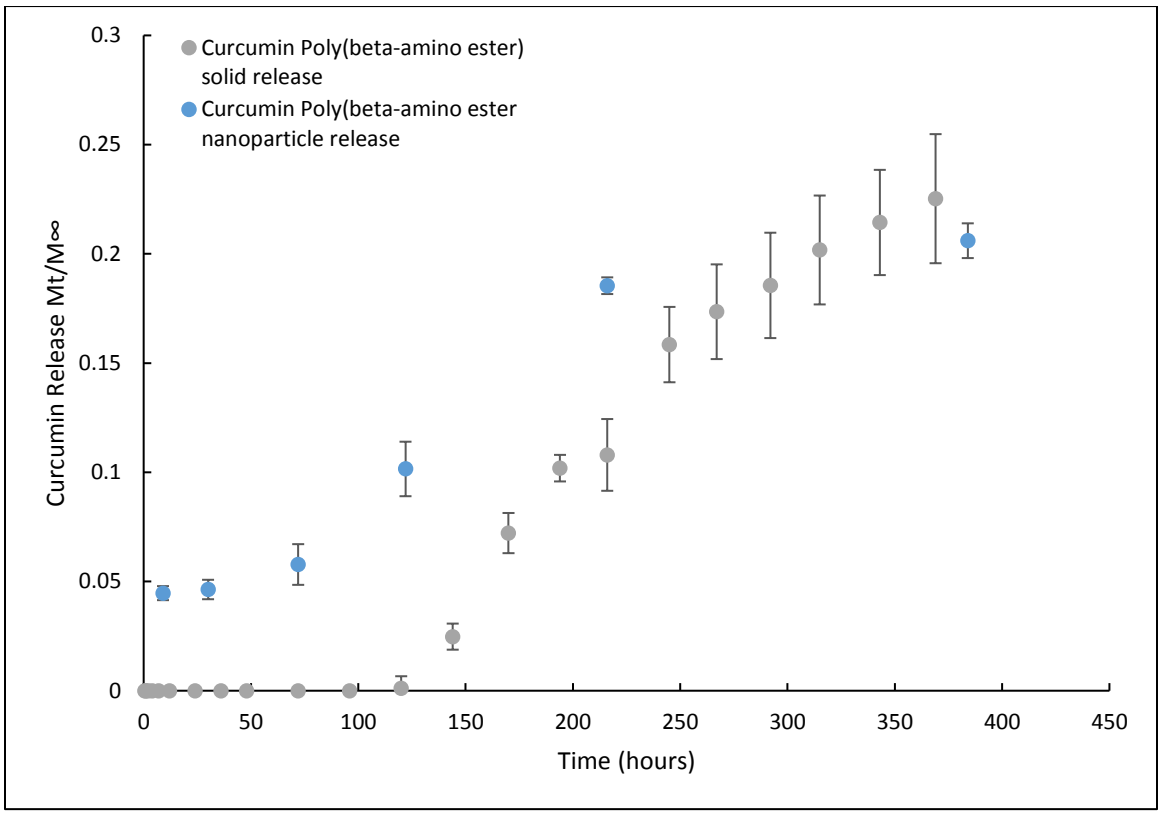

Figure 5-13: Fraction total release of curcumin over time

5.3.4.2 Nanoparticle Curcumin Release HPLC

CPBAE polymer was solubilized in acetone and then added into 0.1wt% SDS PBS for nanoparticle degradation trials. Samples were taken at time points and centrifuged at 10,000 rpm for 5 minutes. The supernatant collected was measured for curcumin content using HPLC. An initial burst release of approximately 1% theoretical maximum curcumin was released. The 108 hour time point was observed to have 7% theoretical maximum release of curcumin. This

value only accounts for the curcumin release elution peak at 8 minutes however, and degradation products contain a curcumin and curcuminoid peak. This curcuminoid peak at 11 minutes elution time would add to the curcumin release intensity in UV Vis, but does not contribute when specifically measuring curcumin release in HPLC. This indicates that a significant portion of the polymer does not simply degrade into curcumin. This also shows that a significant portion of other UV-Vis measurements of CPBAE degradation products is from curcuminoids as well as curcumin.

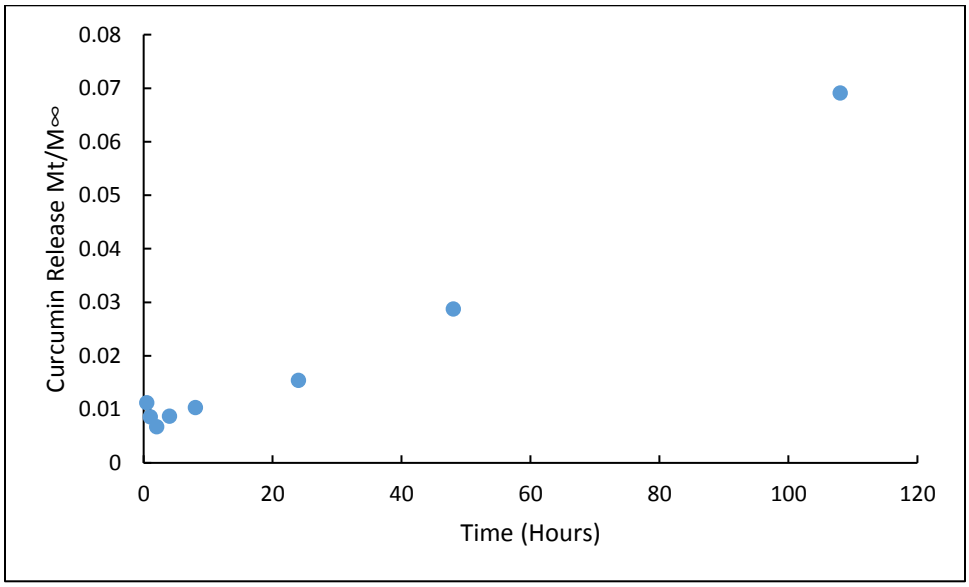

Figure 5-14: Curcumin release from CPBAE over time HPLC integration

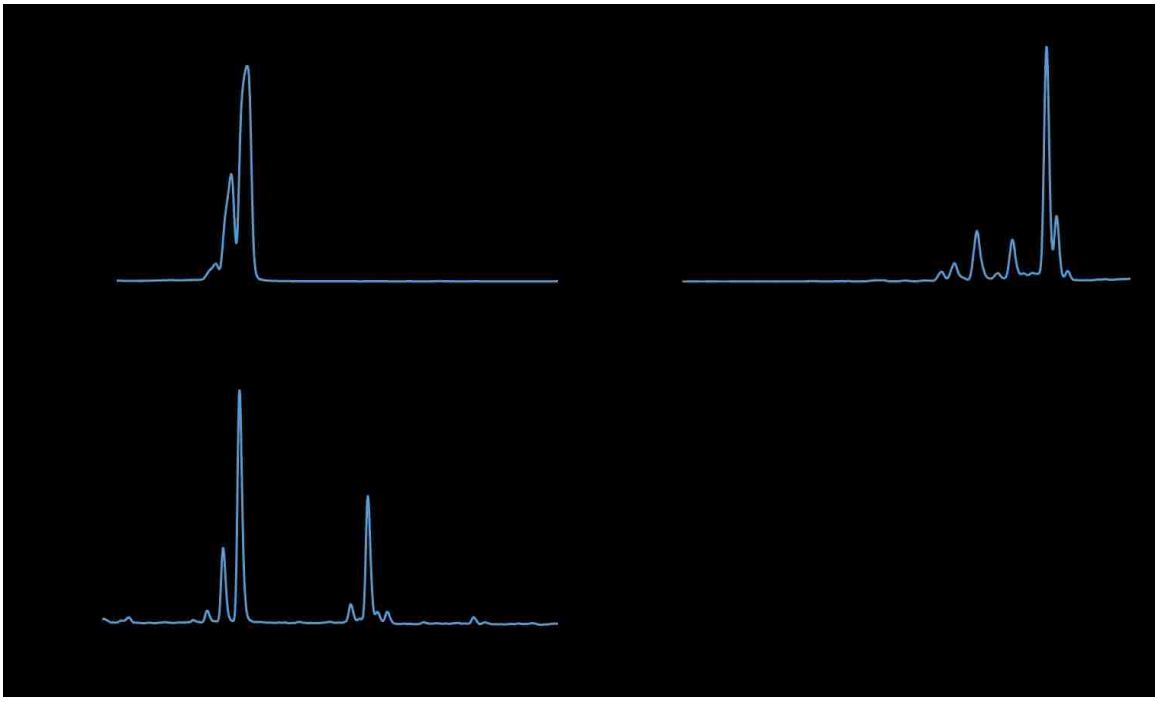

Figure 5-15: HPLC 420nm chromatograms of curcuminoids (A) 100µg/ml Curcumin (B) 100µg/ml CMA (C) 108 hour CPBAE Supernatant

5.3.4.3 Nanoparticle Curcumin Release GPC

CPBAE polymer was solubilized in acetone and then added into 0.1wt% SDS PBS for nanoparticle degradation trials. Samples were taken at time points and centrifuged at 10,000 rpm for 5 minutes. The precipitate was collected to measure molecular weight of the polymer over time. The molecular weight of the CPBAE steadily decreased over time indicating degradation, it only reduces by 50% of its initial molecular weight after 200 hours however. This is indicating that the polymer is not fully breaking down through hydrolytic degradation.

With the similar conditions, CPBAE polymer was solubilized in acetone and then added into 0.1wt% SDS PBS for nanoparticle degradation trials. Samples were taken at time points and the entire solution was freeze dried. The solid recovered after freeze drying was dissolved in THF and characterized through GPC. GPC UV-Vis chromatograms at 420nm were developed for each time point. A polymer peak was observed from 14 to 21 minutes elution time and a low

molecular weight particle peak was observed after 21 minutes. As time goes on in degradation, the polymer peak decreases in volume while the low molecular weight particle peak increases in volume. This trend is captured by graphing the percentage of total volume that the curcuminoids in polymer take up of the total curcuminoid volume in the chromatogram at each time point. With no degradation, 93% of the volume of the chromatogram is taken up by polymerized curcuminoids. After 140 hours of degradation, 65% of the chromatogram's volume is occupied by polymerized curcuminoids. This shows similarly that the CPBAE polymer is degrading but not fully in 140 hours.

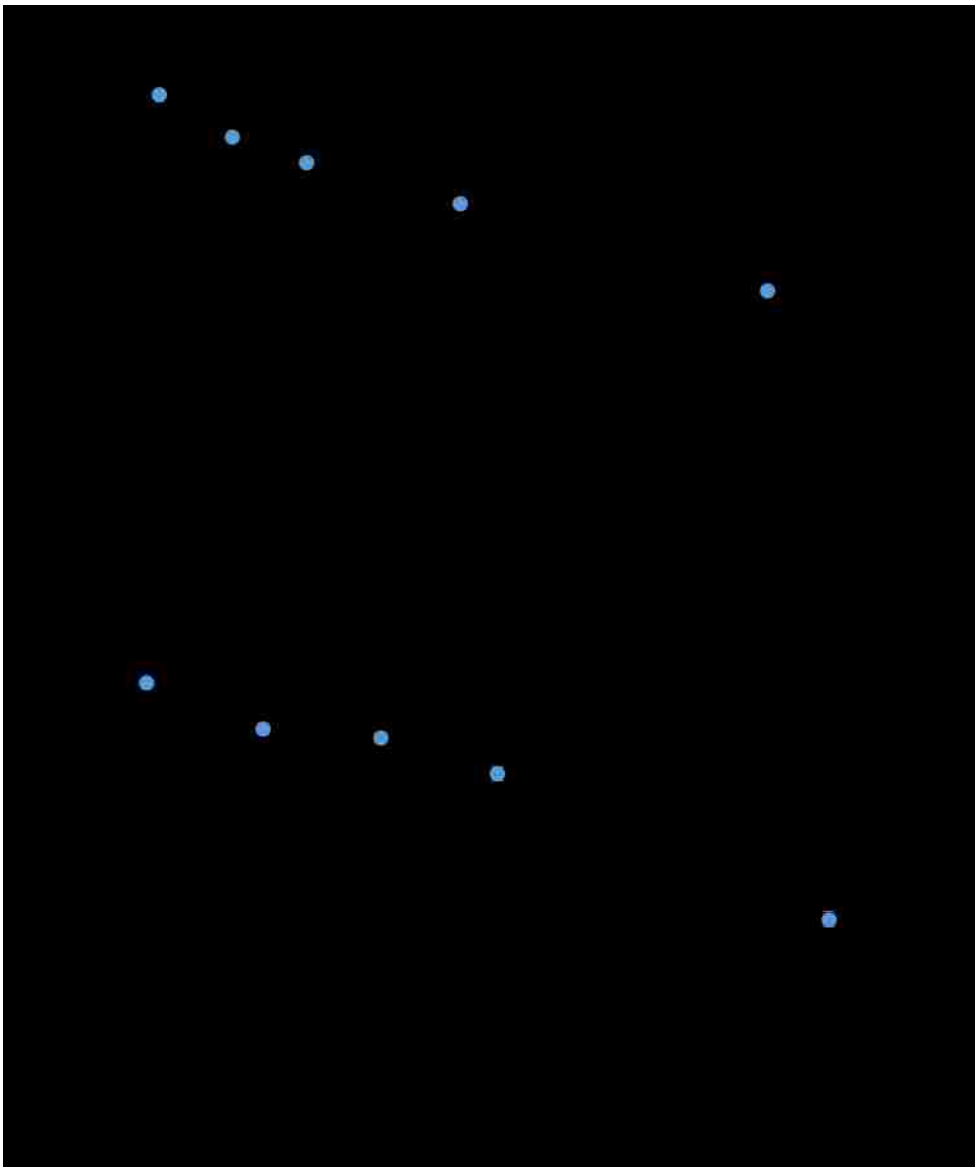

Figure 5-16: GPC assessment of degraded CPBAE molecular weight over time (A) Molecular weight of degraded CPBAE (B) Polymer peak integration GPC 420nm chromatogram

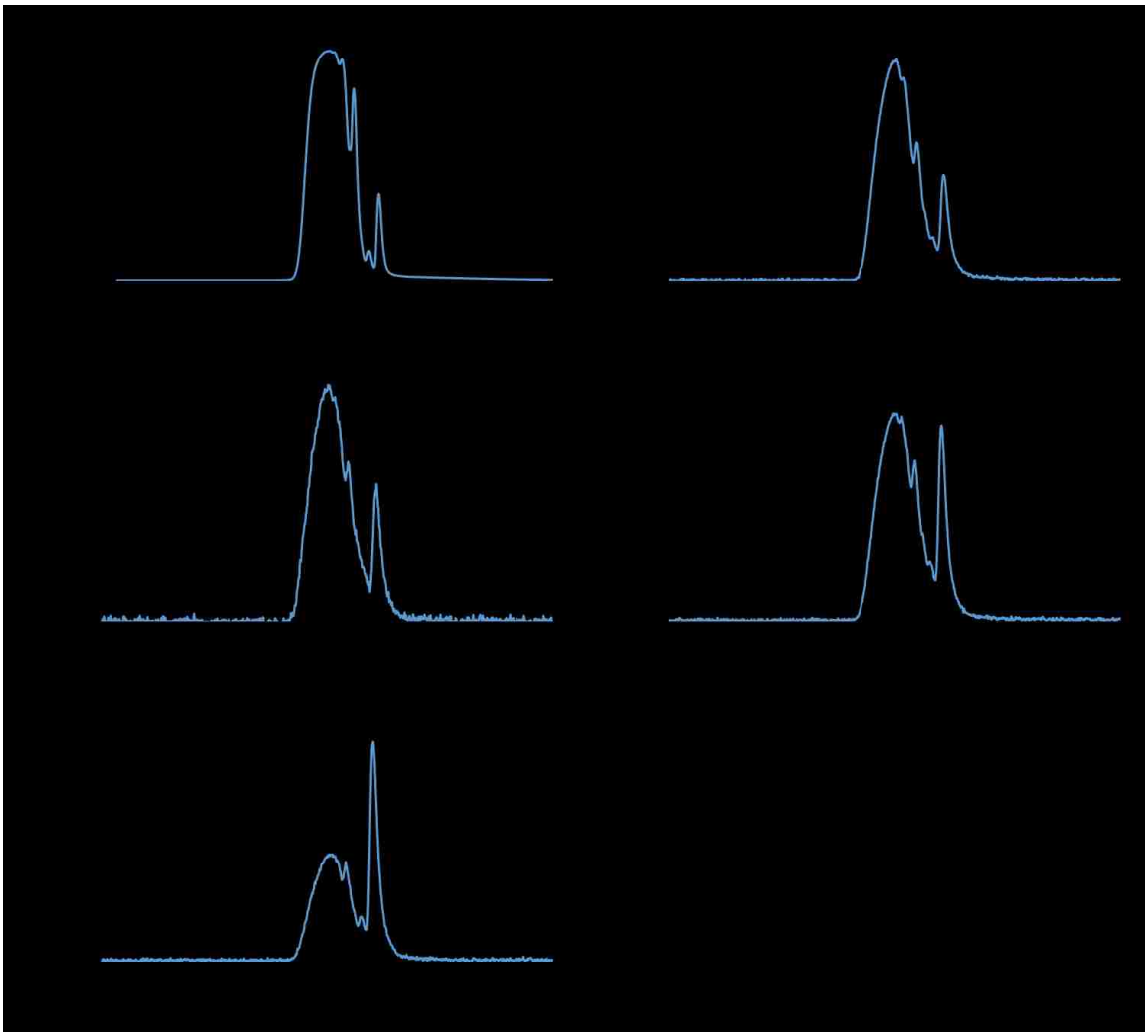

Figure 5-17: CPBAE degradation over time GPC 420nm chromatogram (A) 0 hr (B) 24 hr (C) 48 hr (D) 72 hr (E) 140 hr

5.4 Discussion

The experiments carried out in the chapter were successful in developing a CPBAE polymer that can be formed into nanoparticles through nanoprecipitation and hydrolytically degrade to release curcumin. The nanoparticles were of ideal size for intravenous delivery and had the capability to be coated with antibodies for immunotargeting. Due to inconsistencies in measured release of curcumin from the polymer and the theoretical maximum release of the curcumin though, the structure and purity of the polymer is brought into question. The percent

maximum theoretical release was consistently peaking at 20%. This indicates that the polymer's actual curcumin content is very far from ideal assumptions. Either curcumin is inaccessible from free radical polymerization or the CMA is far from pure. CMA, HPLC and GPC results were the first point of interest. HPLC showed that the CMA did not have any curcumin present but when GPC of the CMA was performed, IR spectra showed a significant amount of material in the 1000-10000 molecular weight elution range, while 420 nm UV-Vis spectra showed that approximately 50% of curcuminoid material was eluted in this high molecular weight peak. This could mean that side reaction in CMA synthesis are polymerizing the monomer. In this case, during CPBAE synthesis the polymerized CMA is not able to react with amines to form a linear polymer.

Another point of friction in examining the polymer was the long degradation time of the polymer. This was not able to be adjusted for though reaction conditions and changing of reactants. Both CMA and IBA were chosen as acrylate and primary amine respectively for the PBAE reaction. Although this system had a high molecular weight, both were very hydrophobic molecules. This leads to the CPBAE degrading much slower than if it had more hydrophilic components. When this tuning was attempted by polymerizing CMA with hydrophilic amines, not reaction occurred. As CMA is a required component for the system and very hydrophobic this limited the options for further adjustment.

5.5 Conclusions

CMA was successfully synthesized and it was confirmed that acrylation took place and no curcumin remained. CPBAE was successfully polymerized using a Michael with curcumin multiacrylate and isobutylamine. This polymer's chemical structure and properties were characterized revealing that significant polymerization was taking place, reaching an average molecular weight of 6000. Nanoparticles of the desired size were produced from the CPBAE and

these were tested for curcumin release through degradation. CPBAE nanoparticles synthesized were able to successfully release curcumin through degradation. The lack of tune-ability of the polymer composition and degradation profile was the greatest detriment.

Chapter 6: Conclusions and Future Directions

Through this project, curcumin has been characterized as a radioprotectant and polymerized to for a degradable delivery system. The *in vitro* effect of curcumin pretreatment on radiation damage on HUVEC was first investigated. The effect of radiation both confluent and proliferating cells was characterized and it was found that even at high doses of radiation, confluent cells showed little reduction in viability, but radiation did inhibit the growth of proliferating HUVECs. From this, a proliferating cell model with a high dose of radiation was utilized for testing. Curcumin was shown to reduce the viability of irradiated cells in a dose dependent manner, while trolox at all concentrations tested had no effect of cell viability. Curcumin and trolox were shown to decrease DCF fluorescence after radiation damage indicating reduction in radiation damage. When the cellular response in cells was evaluated in the γ-H2AX foci Formation Assay, no protection in DNA breaks was found. These results show that antioxidant effect is not protecting cells in this model. This is emphasized by trolox not attenuating radiation damage to cell viability. Curcumin further reduces cell viability as it has been shown to have anti-proliferative effects *in vitro*. This indicates that curcumin's radioprotective effects is not through antioxidant effect directly, rather through its anti-inflammatory properties which are seen *in vivo*. A Michael addition reaction method was used to produce curcumin poly(beta-amino ester). CPBAE was synthesized and characterized. Testing positively indicated polymerization during the reaction. Nanoparticles were synthesized using the developed CPBAE and were able to be size controlled for the desired application of intravenous delivery. Nanoparticles were found to be stable but degraded very slowly through hydrolysis. Both the CPBAE nanoparticles and bulk CPBAE polymer only released a maximum of 20% of the theoretical yield.

Future effort could be put into analyzing the structure of CMA synthesized. The lack of knowledge on the CMA products structure will no doubt cause difficulty when developing future systems. The first step should be to perform chromatography on the CMA and separate the high molecular weight peak and low molecular weight peak. With these samples separated, mass spectrometry and FTIR could be run on each to analyze the structure. This data would dictate future steps in developing a separation of the final CMA product. The simplest way to purify the CMA would be a precipitation and it would work well for bulk material. If no method was feasible, then a more direct chromatography separation would be needed. The peaks are separated distinctly in GPC, but this method does not lend itself well large quantities of material. With a purified CMA, many more options would likely be available for synthesis with other amine and acrylate molecules. This would allow for much greater tuning of both molecular weight and degradation rate of polymer. This would be desirable for developing systems for multiple applications.

Tuning of the radiation model may be necessary to see protective effects of curcumin. 20 Gy of gamma radiation is a very high dose and as seen by the γ-H2AX foci formation assay, this radiation activates close to the maximum number of histones in the assay, thus saturating the test and no protective effect can be seen. At a lower radiation level such as 2 Gy or 5 Gy this damage would not be as great and the saturation would be removed. This would allow protective or damaging effects of curcumin to be measured. It has been difficult to show that curcumin has beneficial effects to radiation damaged cells *in vitro* [97] so this may still not show a benefit. Although an in vitro model tuned to characterize damage will be useful, it may be necessary to test curcumin polymer in an *in vivo* environment to see the full radioprotective effects as vascular permeability and leukocyte recruitment, both of which cannot be represented in a simple *in vitro* model.

References

1. Christensen, D.M., et al., *Management of Ionizing Radiation Injuries and Illnesses, Part 3: Radiobiology and Health Effects of Ionizing Radiation.* The Journal of the American Osteopathic Association, 2014. **114**(7): p. 556-565.
2. Society, A.C., *The Science Behind Radiation Therapy.* 2014.
3. Thariat, J., et al., *Past, present, and future of radiotherapy for the benefit of patients.* Nat Rev Clin Oncol, 2013. **10**(1): p. 52-60.
4. Review, S.C.S., *SEER Stat Fact Sheets: Lung and Bronchus Cancer.* National Cancer Institute, 2016.
5. Kong, F.-M., et al., *Radiation dose effect in locally advanced non-small cell lung cancer.* Journal of Thoracic Disease, 2014. **6**(4): p. 336-347.
6. Oh, Y.-T., et al., *The features of radiation induced lung fibrosis related with dosimetric parameters.* Radiotherapy and Oncology. **102**(3): p. 343-346.
7. Pober, J.S. and W.C. Sessa, *Evolving functions of endothelial cells in inflammation.* Nat Rev Immunol, 2007. **7**(10): p. 803-815.
8. Kumar, V. and A. Abbas, *Inflammation and Repair.* Robbins Basic Pathology, 2012(9th Edition): p. 29-72.
9. Esatbeyoglu, T., et al., *Curcumin—From Molecule to Biological Function.* Angewandte Chemie International Edition, 2012. **51**(22): p. 5308-5332.
10. Vareed, S.K., et al., *Pharmacokinetics of Curcumin Conjugate Metabolites in Healthy Human Subjects.* Cancer epidemiology, biomarkers & prevention : a publication of the American Association for Cancer Research, cosponsored by the American Society of Preventive Oncology, 2008. **17**(6): p. 1411-1417.
11. Storka A, V.B., Klickovic U, Gouya G, Weisshaar S, Aschauer S, Bolger G, Helson L, Wolzt M, *Safety, tolerability and pharmacokinetics of liposomal curcumin in healthy humans.* Int J Clin Pharmacol Ther, 2015. **53**(1): p. 54-65.
12. Naksuriya, O., et al., *Curcumin nanoformulations: A review of pharmaceutical properties and preclinical studies and clinical data related to cancer treatment.* Biomaterials, 2014. **35**(10): p. 3365-3383.
13. Orellana, B.R., et al., *Bioerodible Calcium Sulfate/Poly(β-amino ester) Hydrogel Composites.* Journal of the mechanical behavior of biomedical materials, 2013. **26**: p. 43-53.
14. Zhao, S., et al., *pH-Sensitive Docetaxel-Loaded d-α-Tocopheryl Polyethylene Glycol Succinate–Poly(β-amino ester) Copolymer Nanoparticles for Overcoming Multidrug Resistance.* Biomacromolecules, 2013. **14**(8): p. 2636-2646.
15. Moghimi, S.M. and J. Szebeni, *Stealth liposomes and long circulating nanoparticles: critical issues in pharmacokinetics, opsonization and protein-binding properties.* Progress in Lipid Research, 2003. **42**(6): p. 463-478.
16. Wiewrodt, R., et al., *Size-dependent intracellular immunotargeting of therapeutic cargoes into endothelial cells.* Blood, 2002. **99**(3): p. 912-922.
17. Muro, S., et al., *Slow intracellular trafficking of catalase nanoparticles targeted to ICAM-1 protects endothelial cells from oxidative stress.* American Journal of Physiology - Cell Physiology, 2003. **285**(5): p. C1339-C1347.
18. McMurry, J. and R. Fay, *Nuclear Chemistry.* Chemistry, 2008(5): p. 923-926.
19. *Nuclear Structure and Decay Data.* IAEA Nuclear Data Section, 2016.

20. Son, Y., et al., *The ameliorative effect of silibinin against radiation-induced lung injury: protection of normal tissue without decreasing therapeutic efficacy in lung cancer.* BMC Pulmonary Medicine, 2015. **15**: p. 68.
21. Delgado, O., et al., *Radiation-enhanced Lung Cancer Progression in a Transgenic Mouse Model of Lung Cancer is Predictive of Outcomes in Human Lung and Breast Cancer.* Clinical cancer research : an official journal of the American Association for Cancer Research, 2014. **20**(6): p. 1610-1622.
22. Cho, Y.J., et al., *Curcumin Attenuates Radiation-Induced Inflammation and Fibrosis in Rat Lungs.* The Korean Journal of Physiology & Pharmacology : Official Journal of the Korean Physiological Society and the Korean Society of Pharmacology, 2013. **17**(4): p. 267-274.
23. Lee, J.C., et al., *Dietary Curcumin Increases Antioxidant Defenses in Lung, Ameliorates Radiation-Induced Pulmonary Fibrosis, and Improves Survival in Mice.* Radiation research, 2010. **173**(5): p. 590-601.
24. Bucci, M.K., A. Bevan, and M. Roach, *Advances in Radiation Therapy: Conventional to 3D, to IMRT, to 4D, and Beyond.* CA: A Cancer Journal for Clinicians, 2005. **55**(2): p. 117-134.
25. Tipton KN, S.N., Bruening W, et al. , *Stereotactic Body Radiation Therapy.* Agency for Healthcare Research and Quality (US) Comparative Effectiveness Technical Briefs, 2011. **6**.
26. Lemjabbar-Alaoui, H., et al., *Lung cancer: Biology and treatment options.* Biochimica et Biophysica Acta (BBA) - Reviews on Cancer, 2015. **1856**(2): p. 189-210.
27. Gustafsson, B.I., et al., *Bronchopulmonary neuroendocrine tumors.* Cancer, 2008. **113**(1): p. 5-21.
28. Rudin, C.M., et al., *Treatment of Small-Cell Lung Cancer: American Society of Clinical Oncology Endorsement of the American College of Chest Physicians Guideline.* Journal of Clinical Oncology, 2015. **33**(34): p. 4106-4111.
29. Wang, J., et al., *Comparison of Clinical Outcomes of VATS and SBRT in the Treatment of NSCLC.* Chinese Journal of Lung Cancer; Vol 19, No 3 (2016): Chinese Journal of Lung Cancer, 2016.
30. Oh, Y.-T., et al., *The features of radiation induced lung fibrosis related with dosimetric parameters.* Radiotherapy and Oncology, 2012. **102**(3): p. 343-346.
31. Giuliani, M.E., et al., *Correlation of Dosimetric and Clinical Factors With the Development of Esophagitis and Radiation Pneumonitis in Patients With Limited-Stage Small-Cell Lung Carcinoma.* Clinical Lung Cancer. **16**(3): p. 216-220.
32. Seppenwoolde, Y., et al., *Comparing different NTCP models that predict the incidence of radiation pneumonitis.* International Journal of Radiation Oncology*Biology*Physics, 2003. **55**(3): p. 724-735.
33. Kong, F.-M., et al., *Final toxicity results of a radiation-dose escalation study in patients with non–small-cell lung cancer (NSCLC): Predictors for radiation pneumonitis and fibrosis.* International Journal of Radiation Oncology*Biology*Physics, 2006. **65**(4): p. 1075-1086.
34. Testolin, A., et al., *Stereotactic body radiation therapy for a new lung cancer arising after pneumonectomy: dosimetric evaluation and pulmonary toxicity.* The British Journal of Radiology, 2015. **88**(1055): p. 20150228.
35. Macdonald, J., H.F. Galley, and N.R. Webster, *Oxidative stress and gene expression in sepsis.* British Journal of Anaesthesia, 2003. **90**(2): p. 221-232.
36. Amelia, C., *Cell Responses to Oxidative Stressors.* Current Pharmaceutical Design, 2010. **16**(12): p. 1387-1395.

37. B, H., *Free radicals, antioxidants, and human disease: curiosity, cause, or consequence?* The Lancet, 1994. **344**(8924): p. 721-724.
38. Dalleau, S., et al., *Cell death and diseases related to oxidative stress:4-hydroxynonenal (HNE) in the balance.* Cell Death Differ, 2013. **20**(12): p. 1615-1630.
39. Ogasawara, M.A. and H. Zhang, *Redox Regulation and Its Emerging Roles in Stem Cells and Stem-Like Cancer Cells.* Antioxidants & Redox Signaling, 2009. **11**(5): p. 1107-1122.
40. FREI, B., *Molecular and biological mechanisms of antioxidant action.* The FASEB Journal, 1999. **13**(9): p. 963-964.
41. Terasaki, Y., et al., *Hydrogen therapy attenuates irradiation-induced lung damage by reducing oxidative stress.* American Journal of Physiology - Lung Cellular and Molecular Physiology, 2011. **301**(4): p. L415-L426.
42. Wattamwar, P.P., et al., *Antioxidant Activity of Degradable Polymer Poly(trolox ester) to Suppress Oxidative Stress Injury in the Cells.* Advanced Functional Materials, 2010. **20**(1): p. 147-154.
43. Gardi, C., et al., *Quercetin reduced inflammation and increased antioxidant defense in rat adjuvant arthritis.* Archives of Biochemistry and Biophysics, 2015. **583**: p. 150-157.
44. *Protective effects of Quercetin and chronic moderate exercise (training) against oxidative stress in the liver tissue of streptozotocin-induced diabetic rats.* Acta Physiologica Hungarica, 2016. **103**(1): p. 49-64.
45. Boydens, C., et al., *Relaxant and Antioxidant Capacity of the Red Wine Polyphenols, Resveratrol and Quercetin, on Isolated Mice Corpora Cavernosa.* The Journal of Sexual Medicine, 2015. **12**(2): p. 303-312.
46. Tamaki, N., et al., *Resveratrol improves oxidative stress and prevents the progression of periodontitis via the activation of the Sirt1/AMPK and the Nrf2/antioxidant defense pathways in a rat periodontitis model.* Free Radical Biology and Medicine, 2014. **75**: p. 222-229.
47. Bhandarkar, S.S. and J.L. Arbiser, *CURCUMIN AS AN INHIBITOR OF ANGIOGENESIS*, in *The Molecular Targets and Therapeutic Uses of Curcumin in Health and Disease*, B.B. Aggarwal, Y.-J. Surh, and S. Shishodia, Editors. 2007, Springer US: Boston, MA. p. 185-195.
48. Motterlini, R., et al., *Curcumin, an antioxidant and anti-inflammatory agent, induces heme oxygenase-1 and protects endothelial cells against oxidative stress.* Free Radical Biology and Medicine, 2000. **28**(8): p. 1303-1312.
49. Naksuriya, O. and S. Okonogi, *Comparison and combination effects on antioxidant power of curcumin with gallic acid, ascorbic acid, and xanthone.* Drug Discoveries & Therapeutics, 2015. **9**(2): p. 136-141.
50. Singh, S. and B.B. Aggarwal, *Activation of Transcription Factor NF-κB Is Suppressed by Curcumin (Diferuloylmethane).* Journal of Biological Chemistry, 1995. **270**(42): p. 24995-25000.
51. Sankar Ghosh, a. Michael J. May, and E.B. Kopp, *NF-κB AND REL PROTEINS: Evolutionarily Conserved Mediators of Immune Responses.* Annual Review of Immunology, 1998. **16**(1): p. 225-260.
52. Ghosh, S. and M.S. Hayden, *New regulators of NF-[kappa]B in inflammation.* Nat Rev Immunol, 2008. **8**(11): p. 837-848.
53. P, G., *Essentials of pathology for toxicologists.* CRC Press, 2002.
54. Wolff, B., et al., *Endothelial Cell "Memory" of Inflammatory Stimulation: Human Venular Endothelial Cells Store Interleukin 8 in Weibel-Palade Bodies.* The Journal of Experimental Medicine, 1998. **188**(9): p. 1757-1762.

55. Bevilacqua, M.P., et al., *Interleukin 1 acts on cultured human vascular endothelium to increase the adhesion of polymorphonuclear leukocytes, monocytes, and related leukocyte cell lines.* Journal of Clinical Investigation, 1985. **76**(5): p. 2003-2011.
56. Cao, Q., D.C.H. Harris, and Y. Wang, *Macrophages in Kidney Injury, Inflammation, and Fibrosis.* Physiology, 2015. **30**(3): p. 183-194.
57. Kastellorizios, M., N. Tipnis, and D.J. Burgess, *Foreign Body Reaction to Subcutaneous Implants*, in *Immune Responses to Biosurfaces: Mechanisms and Therapeutic Interventions*, D.J. Lambris, et al., Editors. 2015, Springer International Publishing: Cham. p. 93-108.
58. Omarini, C., E. Thanopoulou, and S.R.D. Johnston, *Pneumonitis and pulmonary fibrosis associated with breast cancer treatments.* Breast Cancer Research and Treatment, 2014. **146**(2): p. 245-258.
59. Abe, Y., S.H.U. Hashimoto, and T. Horie, *CURCUMIN INHIBITION OF INFLAMMATORY CYTOKINE PRODUCTION BY HUMAN PERIPHERAL BLOOD MONOCYTES AND ALVEOLAR MACROPHAGES.* Pharmacological Research, 1999. **39**(1): p. 41-47.
60. Zhao, X., et al., *Doxorubicin and curcumin co-delivery by lipid nanoparticles for enhanced treatment of diethylnitrosamine-induced hepatocellular carcinoma in mice.* European Journal of Pharmaceutics and Biopharmaceutics, 2015. **93**: p. 27-36.
61. Kang, J.H., et al., *Curcumin sensitizes human lung cancer cells to apoptosis and metastasis synergistically combined with carboplatin.* Experimental Biology and Medicine, 2015. **240**(11): p. 1416-1425.
62. Qian, Y., et al., *Curcumin Enhances the Radiosensitivity of U87 Cells by Inducing DUSP-2 Up-Regulation.* Cellular Physiology and Biochemistry, 2015. **35**(4): p. 1381-1393.
63. Chiang, I., Liu, Y., Hsu, F., Chien, Y., Kao, C. K., Lin, W., Chung, J., Hwang, J., *Curcumin synergistically enhances the radiosensitivity of human oral squamous cell carcinoma via suppression of radiation-induced NF-κB activity.* Oncology Reports, 2014. **31**(4): p. 1729-1737.
64. Shehzad, A., et al., *Curcumin induces radiosensitivity of in vitro and in vivo cancer models by modulating pre-mRNA processing factor 4 (Prp4).* Chemico-Biological Interactions, 2013. **206**(2): p. 394-402.
65. Sahin, K., et al., *Comparative In Vivo Evaluations of Curcumin and Its Analog Difluorinated Curcumin Against Cisplatin-Induced Nephrotoxicity.* Biological Trace Element Research, 2014. **157**(2): p. 156-163.
66. Bollimpelli, V.S., et al., *Neuroprotective effect of curcumin-loaded lactoferrin nano particles against rotenone induced neurotoxicity.* Neurochemistry International, 2016. **95**: p. 37-45.
67. Sa, G. and T. Das, *Anti cancer effects of curcumin: cycle of life and death.* Cell Division, 2008. **3**: p. 14-14.
68. Das, T., et al., *Multifocal signal modulation therapy of cancer: ancient weapon, modern targets.* Molecular and Cellular Biochemistry, 2010. **336**(1): p. 85-95.
69. Kunnumakkara, A.B., P. Anand, and B.B. Aggarwal, *Curcumin inhibits proliferation, invasion, angiogenesis and metastasis of different cancers through interaction with multiple cell signaling proteins.* Cancer Letters. **269**(2): p. 199-225.
70. Shishodia, S., T. Singh, and M.M. Chaturvedi, *MODULATION OF TRANSCRIPTION FACTORS BY CURCUMIN*, in *The Molecular Targets and Therapeutic Uses of Curcumin in Health and Disease*, B.B. Aggarwal, Y.-J. Surh, and S. Shishodia, Editors. 2007, Springer US: Boston, MA. p. 127-148.

71. Cheng AL, H.C., Lin JK, Hsu MM, Ho YF, Shen TS, Ko JY, Lin JT, Lin BR, Ming-Shiang W, Yu HS, Jee SH, Chen GS, Chen TM, Chen CA, Lai MK, Pu YS, Pan MH, Wang YJ, Tsai CC, Hsieh CY, *Phase I clinical trial of curcumin, a chemopreventive agent, in patients with high-risk or pre-malignant lesions.* Anticancer Res, 2001. **21**(4B): p. 2895-2900.
72. Anand, P., et al., *Bioavailability of Curcumin: Problems and Promises.* Molecular Pharmaceutics, 2007. **4**(6): p. 807-818.
73. Mohanty, C., M. Das, and S.K. Sahoo, *Emerging role of nanocarriers to increase the solubility and bioavailability of curcumin.* Expert Opinion on Drug Delivery, 2012. **9**(11): p. 1347-1364.
74. Hwang, I.-T.C.Y.-C.L.F.-T.H.Y.-C.C.C.-H.K.K.W.-J.L.J.-G.C.J.-J., *Curcumin synergistically enhances the radiosensitivity of human oral squamous cell carcinoma via suppression of radiation-induced NF-κB activity.* Oncology Reports, 2014. **31**(4): p. 1729-1737.
75. Qiao, Q., Y. Jiang, and G. Li, *Inhibition of the PI3K/AKT-NF-κB Pathway With Curcumin Enhanced Radiation-Induced Apoptosis in Human Burkitt's Lymphoma.* Journal of Pharmacological Sciences, 2013. **121**(4): p. 247-256.
76. VEERARAGHAVAN, J., et al., *Curcumin-altered p53-Response Genes Regulate Radiosensitivity in p53-Mutant Ewing's Sarcoma Cells.* Anticancer Research, 2010. **30**(10): p. 4007-4015.
77. Akpolat, M., M. Kanter, and M.C. Uzal, *Protective effects of curcumin against gamma radiation-induced ileal mucosal damage.* Archives of Toxicology, 2009. **83**(6): p. 609-617.
78. Tawfik, S.S., A.M. Abouelella, and Y.E. Shahein, *Curcumin protection activities against γ-Rays-induced molecular and biochemical lesions.* BMC Research Notes, 2013. **6**: p. 375-375.
79. Özgen, S.Ç., et al., *The Protective Effect of Curcumin on Ionizing Radiation-induced Cataractogenesis in Rats.* Balkan medical journal, 2012. **29**(4): p. 358-363.
80. Shi, H.-s., et al., *A systemic administration of liposomal curcumin inhibits radiation pneumonitis and sensitizes lung carcinoma to radiation.* International Journal of Nanomedicine, 2012. **7**: p. 2601-2611.
81. Aktas, C., M. Kanter, and Z. Kocak, *Antiapoptotic and proliferative activity of curcumin on ovarian follicles in mice exposed to whole body ionizing radiation.* Toxicology and Industrial Health, 2012. **28**(9): p. 852-63.
82. Ryan, J.L., et al., *Curcumin for Radiation Dermatitis: A Randomized, Double-Blind, Placebo-Controlled Clinical Trial of Thirty Breast Cancer Patients.* Radiation research, 2013. **180**(1): p. 34-43.
83. Anderson, D.G., D.M. Lynn, and R. Langer, *Semi-Automated Synthesis and Screening of a Large Library of Degradable Cationic Polymers for Gene Delivery.* Angewandte Chemie International Edition, 2003. **42**(27): p. 3153-3158.
84. Akinc, A., et al., *Synthesis of Poly(β-amino ester)s Optimized for Highly Effective Gene Delivery.* Bioconjugate Chemistry, 2003. **14**(5): p. 979-988.
85. Lynn, D.M. and R. Langer, *Degradable Poly(β-amino esters): Synthesis, Characterization, and Self-Assembly with Plasmid DNA.* Journal of the American Chemical Society, 2000. **122**(44): p. 10761-10768.
86. Anderson, D.G., et al., *A Combinatorial Library of Photocrosslinkable and Degradable Materials.* Advanced Materials, 2006. **18**(19): p. 2614-2618.
87. Shenoy, D., et al., *Poly(Ethylene Oxide)-Modified Poly(β-Amino Ester) Nanoparticles as a pH-Sensitive System for Tumor-Targeted Delivery of Hydrophobic Drugs: Part I. In Vitro Evaluations.* Molecular pharmaceutics, 2005. **2**(5): p. 357-366.

88. Lo, S.S., et al., *Stereotactic body radiation therapy: a novel treatment modality.* Nat Rev Clin Oncol, 2010. **7**(1): p. 44-54.
89. Tsoutsou, P.G. and M.I. Koukourakis, *Radiation pneumonitis and fibrosis: Mechanisms underlying its pathogenesis and implications for future research.* International Journal of Radiation Oncology*Biology*Physics, 2006. **66**(5): p. 1281-1293.
90. Cannon, D.M., et al., *Dose-Limiting Toxicity After Hypofractionated Dose-Escalated Radiotherapy in Non–Small-Cell Lung Cancer.* Journal of Clinical Oncology, 2013. **31**(34): p. 4343-4348.
91. Terakedis, B. and W. Sause, *Radiation Dose Escalation in Stage III Non-Small-Cell Lung Cancer.* Frontiers in Oncology, 2011. **1**: p. 47.
92. Kouvaris, J.R., V.E. Kouloulias, and L.J. Vlahos, *Amifostine: The First Selective-Target and Broad-Spectrum Radioprotector.* The Oncologist, 2007. **12**(6): p. 738-747.
93. Koukourakis, M.I.M.K., George MD; Panteliadou, Marianthi MD; Papadopoulou, Aikaterini MD; Tsiarkatsi, Maria BSN; Papachristou, Eli BSN; Bebeli, Maria BSN, *Dose Escalation of Amifostine for Radioprotection During Pelvic Accelerated Radiotherapy.* American Journal of Clinical Oncology, 2013. **36**(4): p. 338-343.
94. Jayam Raviraj, V.K.B., Venkata Suneel Kumar, Uday Shankar Reddy, Venkata Suman, *Radiosensitizers, radioprotectors, and radiation mitigators.* Indian J Dent Res 2014(25): p. 83-90.
95. Seed, T.M., *RADIATION PROTECTANTS: CURRENT STATUS AND FUTURE PROSPECTS.* Health Physics, 2005. **89**(5): p. 531-545.
96. Jagetia, G., *RADIOPROTECTION AND RADIOSENSITIZATION BY CURCUMIN*, in *The Molecular Targets and Therapeutic Uses of Curcumin in Health and Disease*, B. Aggarwal, Y.-J. Surh, and S. Shishodia, Editors. 2007, Springer US. p. 301-320.
97. Gautam, S.C., et al., *Nonselective Inhibition of Proliferation of Transformed and Nontransformed Cells by the Anticancer Agent Curcumin (Diferuloylmethane).* Biochemical Pharmacology, 1998. **55**(8): p. 1333-1337.
98. Wahlstrom, B. and G. Blennow, *A study on the fate of curcumin in the rat.* Acta Pharmacol, 1978. **43**(2): p. 86-92.
99. Shoba, G., et al., *Influence of Piperine on the Pharmacokinetics of Curcumin in Animals and Human Volunteers.* Planta Med, 1998. **64**(04): p. 353-356.
100. Hoehle, S.I., et al., *Metabolism of Curcuminoids in Tissue Slices and Subcellular Fractions from Rat Liver.* Journal of Agricultural and Food Chemistry, 2006. **54**(3): p. 756-764.
101. Ravindranath, V. and N. Chandrasekhara, *Metabolism of curcumin—studies with [3H]curcumin.* Toxicology 1981. **22**(4): p. 337-344.
102. Li, L., F.S. Braiteh, and R. Kurzrock, *Liposome-encapsulated curcumin.* Cancer, 2005. **104**(6): p. 1322-1331.
103. Kunwar, A., et al., *Transport of liposomal and albumin loaded curcumin to living cells: An absorption and fluorescence spectroscopic study.* Biochimica et Biophysica Acta (BBA) - General Subjects, 2006. **1760**(10): p. 1513-1520.
104. Mosley, C.A., D.C. Liotta, and J.P. Snyder, *HIGHLY ACTIVE ANTICANCER CURCUMIN ANALOGUES*, in *The Molecular Targets and Therapeutic Uses of Curcumin in Health and Disease*, B.B. Aggarwal, Y.-J. Surh, and S. Shishodia, Editors. 2007, Springer US: Boston, MA. p. 77-103.
105. Bisht, S., et al., *Polymeric nanoparticle-encapsulated curcumin ("nanocurcumin"): a novel strategy for human cancer therapy.* Journal of Nanobiotechnology, 2007. **5**: p. 3-3.

VITA

Mark Cheyne Bailey

Born Bedford Park, SA Australia

Education

B.S. Biomedical Engineering , Summa Cum Laude 2013
Minor in Math and Physics, da Vinci Certificate in Product Innovation
Virginia Commonwealth University, Richmond, VA

Professional Positions

Graduate TA and RA, *University of Kentucky* 2013-2015
STEM Ambassador, *Science Museum of Virginia* 2013
Undergraduate RA, *Virginia Commonwealth University* 2013
Da Vinci Project Team member, *Virginia Commonwealth University and Pfizer Consumer Healthcare* 2012
Research Experience for Undergraduates, *University of Kentucky* 2011

Publications

C. Jordan, V. V. Shuvaev, M. Bailey, V. R. Muzykantov, T. D. Dziubla, *The Role of Carrier Geometry in Overcoming Biological Barriers to Drug Delivery.* Current Pharmaceutical Design, 2016. **22**(9): p. 1259-1273.

Poster Presentations

Society for Biomaterials Fall Symposium 2014
American Institute of Chemical Engineers National Student Conference 2011